



**Innovative analytical and
process solutions for cosmetics**

Analytical and process solutions for cosmetics industry

Key words

Continuous Processing, Compounding, Extrusion, Rheology, Molecular Spectroscopy, New Formulation, Texture, Structure, Consumer Perception, Quality Control

Introduction

The highly innovative cosmetics and personal care products industry strives to deliver effective products that are both appealing and safe for consumers. Scientific strength and advancements often help determine who succeeds in such a competitive environment.

Finding and integrating simpler, sustainable production techniques is key as many of the actual production processes are lengthy and highly sophisticated (up to 30 different steps). There is also a demand in today's market for natural and organic cosmetics with basic, traditional ingredients and herbs; such products can be challenging to produce. In addition, there are high requirements within Europe for the assessment of safety and good manufacturing as well as notification obligations for manufacturers and importers. New process and hyphenated approaches help cosmetics producers overcome such challenges.

Twin screw extruders used in hot melt extrusion (HME) or in a continuous granulation process enable the development of new formulations and new textures. Transitioning from batch to continuous processing also increases productivity by reducing the repetitive steps of milling and blending, and by offering rules for scale up.

Molecular spectroscopy – namely FTIR, NIR and Raman spectroscopy – offers a direct way to understand the molecular structure of substances, which helps in testing the quality of educts and products. Identifying the molecular changes of a substance under shear stress, during temperature change or after UV exposure allows scientists to better understand a product and predict its behavior during consumer use.

Rheological testing provides comprehensive tools for the cosmetics industry to support new product development. It's particularly useful in improving processing conditions as well as for quality control of intermediates and finished products. Customer expectations and consumer perceptions toward texture, sensorial experience, spreadability and the general flow behavior of a product can easily be assessed by measurable rheological parameters. Rheological tests also allow for the prediction of shelf stability and the establishment of structure/property relationships which can be even more revealing when used simultaneously with complementary analytical methods such as molecular spectroscopy.

It's critical to understand what to measure in formulation development and quality control for cosmetics and personal care products, and which tools are best to do it. This collection of application notes, whitepapers and articles covers various aspects to help you optimize final product properties and processing.

Table of contents

New Formulation Processing / Production

- Extrusion of color cosmetics
- Encapsulation of flavors and ingredients using a twin-screw extruder
- Optimization of the filling process of shampoo sachets with the HAAKE CaBER 1 extensional rheometer
- Classification of herbs by FT-NIR spectroscopy using the Thermo Scientific Antaris II Analyzer

Product Development / Quality Control / Quality Enhancement

- Benefits of hyphenated techniques to understand macroscopic and molecular relations in a process environment
 - Monitoring emulsions morphology under shear via simultaneous rheometry and in-situ FTIR spectroscopy
 - Rheology-Raman spectroscopy: tracking emulsion stability with the combination of a rheometer and Raman spectrometer
 - Stability of cosmetic emulsions quantified with rheology and simultaneous DEA
 - Investigating cocoa butter crystallization using simultaneous rheology and Raman spectroscopy
- The rheological behaviour of shampoos - What makes a product acceptable for a specific target customer?
- Product stability and shelf-life - What rheology has to do with it
- Investigating the viscoelastic behavior of cosmetic emulsions by performing creep and recovery tests
- Performing quality control (QC) tests on cosmetic emulsions with the HAAKE Viscotester iQ rheometer
- Optimization of the filling process of shampoo sachets with the HAAKE CaBER 1 extensional rheometer
- Quality control of industrial dye products using absorbance spectroscopy

Extrusion of color cosmetics

Author

Dirk Leister
Thermo Fisher Scientific, Karlsruhe, Germany

Executive summary

Color cosmetics are a fast-growing segment of the cosmetics and personal care products market. Manufacturers can gain a competitive advantage by developing more new formulations for this segment at a faster pace.

Compounding solutions from Thermo Fisher Scientific can help speed up the process for formulation development of eyeshadow. Utilize a parallel twin-screw extruder to mix powder and liquid ingredients into a homogeneous product within a single process.

The compact design of the Thermo Scientific™ Process 11 Hygienic Extruder allows users to optimize the process and develop new cosmetic formulations on a laboratory scale, with significantly reduced test time, sample size and waste.

The challenge

Within the cosmetics industry, decorative cosmetics are the fastest growing segment. Consumers' desire for new and innovative products has generated a high demand for new mascara, eyeshadow or facial makeup products.

Developing new formulations in batch processes is quite time consuming, requiring repetitive steps of milling and blending until the final product homogeneity is achieved.

Transitioning from batch to a continuous process reduces the number process steps and gives a distinct advantage to manufacturers of cosmetic products. The result of such a transition is a more homogeneous product and a larger number of new formulations for the same amount of time spent in the laboratory.

Challenge solved

A twin-screw extruder is an excellent mixing tool as it combines multiple process steps into one continuously operating instrument [1]. Its modularity allows different mixing



Fig 1: Feeding powders and liquid ingredients into the extruder.

zones within the process which can then disperse agglomerates by vigorous mixing or apply gentle blending to more sensitive materials such as pearls.

An eyeshadow formulation usually consists of fillers, absorbents, binders, colorants and preservatives [2]. Most often the pigmented powder products are mixed first with the base material (e.g., talc) for a proper color extension, which sets the appearance that the product will have after the customer has applied it. After having achieved the desired degree of homogeneity in the mix of initial substances, the remaining ingredients are added. The more sensitive components are often mixed mildly toward the end of the process.

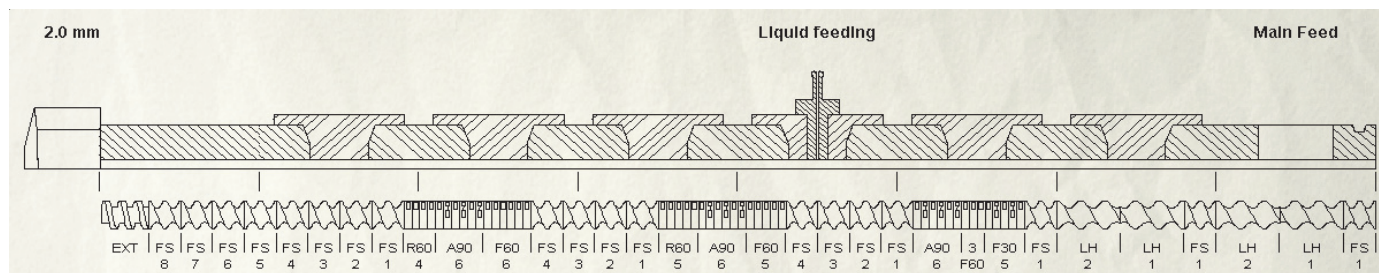


Fig. 2: Barrel and Screw setup.

Fig. 2 shows a typical setup of a screw that has different mixing zones as well as openings along the processing area to introduce ingredients throughout in the process. In addition to powder materials, liquids such as silicone oils may also be added during the compounding process.

At the end of the extruder barrel, a die can be mounted to press the material through giving it a preliminary shape that helps to facilitate the final filling process into godets. Figures 1 and 3 show an example setup of eyeshadow formulation being processed on a Process 11 benchtop twin-screw extruder. The powder and liquid components are mixed continuously within the extruder and the resulting compound is formed by pressing it through a die.

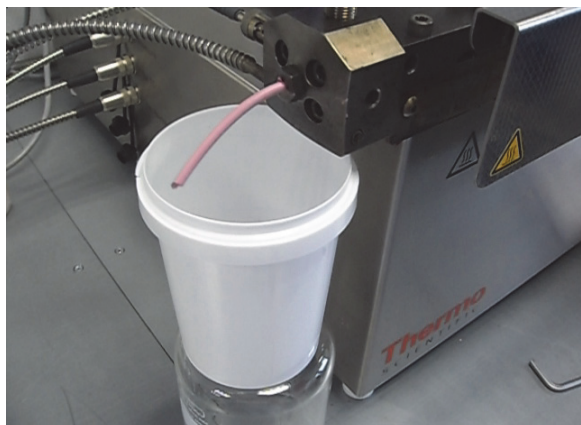


Fig. 3: Pressing the final formulation through a die.

Conclusion

Combining different process steps into one continuously operating instrument, a twin-screw extruder can help significantly speed up formulation development of new makeup products. The precise control of process parameters also mitigates or even eliminates the risk of batch-to-batch variations. The modular setup of the Process 11 instrument helps manufacturers adapt their analyses for different process requirements.

Process 11 Hygienic Extruder:

The Process 11 Hygienic Twin-Screw Extruder has special features and benefits for cosmetic applications:

- Compact bench-top extruder with small footprint
- Intuitive process control via touch screen with data logging
- Allows setup, testing and cleaning by a single user in a laboratory environment
- Eight electric, heated and actively cooled temperature zones for exact temperature control and temperature profiles
- Seven positions along the process to feed multiple components like powders, water, oil or waxes
- Flexible screw design with interchangeable mixing and conveying elements, to optimize the compounding of ingredients
- Suitable for scale-up to industrial production

Further information

We invite you to learn more or contact us to see how we can support you at thermofisher.com/cosmetics.

Resources

- [1] Matthias Jaehrling, "Twin-screw Compounding: Introduction and Scale-up", Webinar, <https://www.thermofisher.com/de/en/home/global/forms/industrial/material-characterization-webinars/twin-screw-compounding-introduction-and-scale-up.html>.
- [2] Baki, G.; Alexander, K.S.; "Introduction to cosmetic formulation and technology", Wiley, [2015]

Find out more at thermofisher.com/cosmetics

ThermoFisher
SCIENTIFIC

Encapsulation of flavors and ingredients using a twin-screw extruder

Authors Authors Authors Authors Authors
Matthias Jährling and Dirk Hauch
Thermo Fisher Scientific, Karlsruhe, Germany

Introduction

Flavors are sensitive and expensive additives used in different industries such as pharmaceutical, chemical, cosmetic and food. Over the last decades these flavors and active ingredients have been encapsulated in a polymeric matrix for various purposes such as protection against oxidation, loss of flavor, taste masking, controlled release, or better product handling.

Possible matrix polymers include starch, different sugars, cellulose derivatives, lipids, proteins and special rubbers. The largest shares have of course starch and sugars. The traditional method of encapsulating flavors is based on a batch process, but it can be improved upon with twin screw melt extrusion.

Traditional processing

The polymers are molten with the addition of water. Then the flavors or active ingredients are added, and mixed by vigorous kneading. Depending on the formulation, excess water may need to be removed under vacuum. Thereafter, the melt is cast as a plate and cooled down.

This process is very cumbersome and time-consuming. Also the required material amount is not flexible because it is predetermined by the size of the batch mixer.

Another popular traditional method for encapsulation of flavors is spray drying. A drawback of this complex, continuous process is the loss of flavors and active ingredients due to high process temperatures. The materials may oxidize, may have a shorter shelf life, and explosion protection measures may even have to be taken for some materials. The high energy consumption for drying in this process also makes it less favorable from an economic standpoint.

Encapsulation using twin-screw melt extrusion

Polymers are frequently processed with extruders, so it is an obvious choice to extend this technology for the encapsulation of flavors.



Fig. 1: Thermo Scientific Process 11 "Hygienic" with face-cut pelletizer.

The flexible combination of dispersive and distributive mixing in a twin-screw extruder is perfectly suitable for continuous encapsulation of flavors. The twin screw extruder allows the temperature to be changed throughout the barrel zones, and it has a modular screw design to induce only the amount of shear and thermal energy needed for the process of encapsulation. This prevents unwanted degradation of the sensitive materials.

In the feeding section of the extruder (see Fig. 2; material flows from right to left) the polymer matrix material is metered and conveyed into the first mixing zone. Due to the heat and shearing, the polymer is transformed into a homogeneous melt. In a secondary feed zone, the flavor is added by means of a liquid feeding pump.

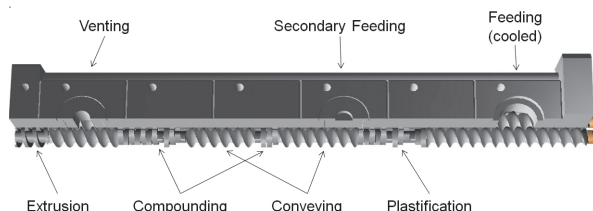


Fig. 2: Schematic of a twin-screw extrusion.

In a further mixing zone, the flavor is now dispersed and evenly distributed into the polymer matrix. At the end of the extruder, the sample pressure is built up to press the compound through a die, and shape it to large number of small strands which are then directly cut into fine pellets by the rotating knife of a face-cut pelletizer. Another option is to extrude the melt directly onto chill-rolls which freeze it down and shape the material into flakes.

The Thermo Scientific™ Process 11 “Hygienic” is the ideal instrument for testing the encapsulation process on a laboratory scale, because it combines the advantages of a compact bench-top extruder, with the full functionality of a production setup. Its modular design enables the optimal adjustment of the extruder barrel and screws to match the application and product needs. All product contact parts are made from stainless, hygienic-grade steel.

As food products are often cleaned with water-based detergents, the high-grade steel provides an advantage over regular extruders which are normally used in polymer processes.

Testing Equipment

- Extrusion System: Process 11 “Hygienic”
- Cooling Circulator:
Thermo Scientific™ Polar Series Accel 500 LC
- Feeder for Premix:
Gravimetric MiniTwin MT0 for Process 11
- Feeder for Liquid:
Thermo Scientific™ Masterflex P/S Pump Systems
- Downstream System: Face-Cut Pelletizer

For an encapsulation of a flavor in a sugar matrix, the Process 11 “Hygienic” equipment setup was designed in a way that the sugar was metered into the cooled, first feeding zone of the extruder, with a gravimetric twin-screw feeder. The sugar was then conveyed by the extruder-screw, into the first mixing zone. There the sugar was molten due to the shear and heat generated by the kneading elements. These kneading elements were followed by conveying screw elements. In a co-rotating twin-screw extruder the conveying elements are not totally filled and the melt is not pressurized. As a result the extruder could be opened again and the flavor was added into the molten sugar by the Masterflex P/S peristaltic pump.

Conveying screw elements then transported the mixture into two subsequent mixing sections, where the flavor was dispersed and evenly distributed in the sugar matrix. At the end of the extruder the pressure was built up, and the final compound was pressed through the die head, into the face-cut pelletizer.

Designing the final product

Fig. 3 shows the final product, collected after cooling in the cyclone of the face-cut pelletizer.

Once the process is developed on the extruder, it is very simple to exchange of the downstream accessories to obtain differently shaped material. Fig. 4 shows flakes produced from the same process using a chill-roll (see Fig. 5) instead of the face-cut pelletizer. The molten material leaving the extruder is compressed and cooled down between two temperature-controlled rolls and formed into a thin sheet. The cooled sheet is then broken down into flakes by a kibbler device at the end of the chill-roll.

Conclusion

Using twin screw extruders for encapsulation of flavors and ingredients into a sugar or polymeric matrix offers several advantages over traditional processes.

The extruder is a continuous working instrument by nature so the amount of end-product is determined by run time and does not require adaptation via different sized production equipment as traditional batch operation does. Compared to the energy-hungry process of spray-drying, extrusion has milder process conditions and reduces the risk of product denaturation.

Finally the choice of downstream equipment (face-cut pelletizing or chill-roll) can help produce application specific end-product as required.

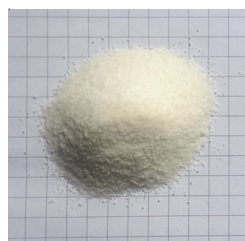


Fig. 3: Encapsulated flavor - pelletized.

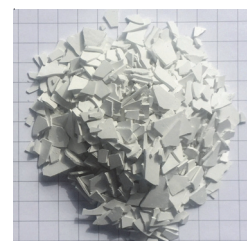


Fig. 4: Encapsulated flavor - pelletized.



Fig. 5: Chill-roll with kibbler.

Find out more at thermofisher.com/extruders

ThermoFisher
SCIENTIFIC

APPLICATION NOTE

Optimization of the filling process of shampoo sachets with the HAAKE CaBER 1 extensional rheometer

Authors

Kevin Barber¹, Alexandra Ewers² and Jint Nijman²

¹Thermo Fisher Scientific, United Kingdom

²Thermo Fisher Scientific, Karlsruhe, Germany

Key words

Shampoo, filling, elongational viscosity, stringiness, HAAKE CaBER

Abstract

With certain shampoo formulations, “strings” of shampoo are formed when filling sachets during production. This causes the product to spill across the sachet seam area. As a consequence, the sachet cannot be properly sealed. Using the Thermo Scientific™ HAAKE™ CaBER™ 1 extensional rheometer “string forming” shampoo formulations were easily and quickly distinguished from “well performing” samples. Rotational rheometers were not able to provide this information.

Introduction

While most commercial rheometers are capable of generating only shear flows, in many industrial processes and applications the flow is predominantly extensional in nature.

Typical examples of this type of flow are fiber spinning, paper coating, extrusion and filling food or toiletries in bottles. This paper describes the optimization of filling shampoo into sachets. With certain shampoo formulations, “strings” of shampoo are formed when filling the sachets, which causes the product to spill across the seam area. As a consequence, the sachet cannot be properly sealed. This failure is expensive as it will result in the disposal of many improperly sealed sachets.

Using classical rotational or oscillatory shear experiments, no discernible differences could be observed between the five shampoo formulations investigated. However, the use of the HAAKE CaBER 1 (Capillary Breakup Extensional Rheometer) allowed the characterization of the formulations’ extensional properties in a quick and easy experiment, thus providing a solution to the problem.

Shampoos usually consist of 80 -90% water, more than 2% detergent, and foaming agents and about 1% of fragrances and preservatives [1]. Often shampoos contain



antistatic agents, thickeners and conditioners [2]. Current health and beauty trends make it important to stabilize special-effect particles in gels, body washes or shampoos. Thickening agents are used to prevent the sedimentation of these particulate phases [3]. However, a problem with thickeners is that they can be the cause of unwanted extensional properties, such as string formation.

These unwanted rheological properties can manifest themselves in an unpleasant and “slimy” feeling while using the product. They can also cause string formation during the high speed filling of a shampoo into sachets or bottles, resulting in improper sealing of the sachet or messy bottles. Slowing down the filling speed would solve the problem, but that has implications for the throughput capability of the production line. A far better solution would be to modify the formulation of the shampoo in such a way that the highest filling speed can be used.

Methods and materials

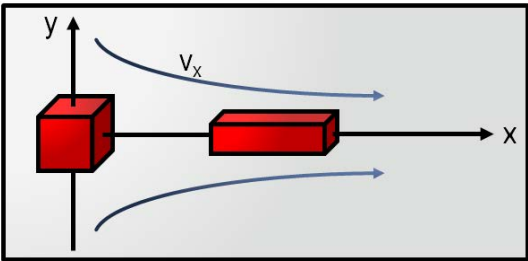
In this investigation five shampoos with different formulations were tested to find out which formulation could be filled into the sachets successfully at a high filling speed.

All formulations were previously tested on a high speed filling line with differing degrees of success. Some exhibited the string formation problem that resulted in failure of the sachet seams.

The measurements were carried out with the HAAKE CaBER 1 extensional rheometer. The CaBER experiment gives a quick insight into the material properties under an extensional deformation which occur, for example, during the sachet filling. It is impossible to determine the extensional properties of a fluid by using a traditional rotational rheometer.

In an extensional flow the stream-lines converge and the velocity increase (i.e. the acceleration) is in the direction of the flow (Figure 1a). This in contrast to the situation in a shear flow where the streamlines are parallel and the velocity increase is perpendicular to the direction of the flow (Figure 1b).

a)



b)

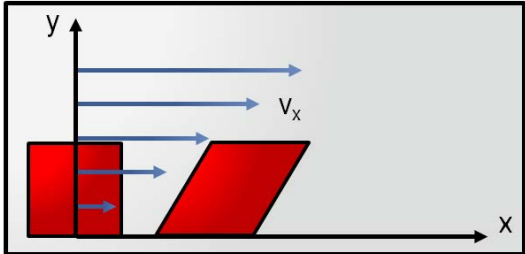


Fig. 1: Comparison between extensional flow (a) and shear flow (b).

The principle of the CaBER experiment is simple. A small quantity of sample (less than 0.2 ml) is placed between two parallel plates (diameter e.g. 6 mm). The fluid is then exposed to a rapid extensional step strain by moving the upper plate upwards, thereby forming a fluid filament (Figure 2). The filament evolution as a function of time is controlled by the balance of the surface tension and the viscous and elastic forces.



Fig. 2: Sequence of a CaBER measurement.



HAAKE CaBER 1 extensional rheometer.

The surface tension is trying to “pinch off” the filament while the extensional rheological properties of the fluid are trying to prevent that. A laser micrometer measures the midpoint diameter of the gradually thinning fluid filament after the upper plate has reached its final position (Figure 3).

From the measured data, which describes the evolution of the filament diameter as a function of time (Figures 2a, 2b and 2c), the filament break-up time (Figure 2d), the extensional deformation, deformation rate and the apparent extensional viscosity can be calculated.

Results and discussions

Five different shampoo samples were tested. Two of the samples (samples 1 and 2), performed well in the sachet filling equipment; the three other samples (samples 3, 4 and 5) did not perform well.

When measured in a rotational rheometer, the five samples did not show any significant differences in the flow curves that would explain their different during the filling of the sachets (Figure 4).

In contrast, when exposed to an extensional flow fluid using the HAAKE CaBER 1 rheometer, the measured diameter versus time curves (see Figure 5) of the five samples nicely rank according to their filling behavior: the shorter the filament lifetime in the CaBER experiment, the better the filling properties.

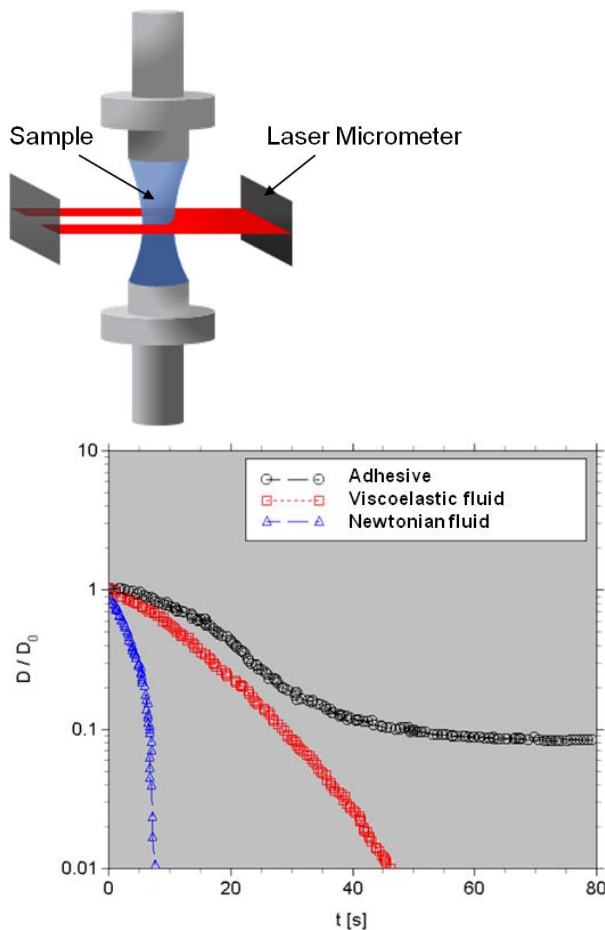


Fig. 3: Principle of the CaBER experiment.

The 5 samples clearly differentiated in their extensional flow properties. The filament lifetimes of the shampoos 1 and 2 are relatively short. These shampoos can be filled into sachets without any obvious problems. For the shampoos 3, 4 and 5, the filament lifetimes are significantly longer, which leads to problems in sachet filling. String formations prevented the sachets sealing, a problem which can only be resolved by slowing down the filling process.

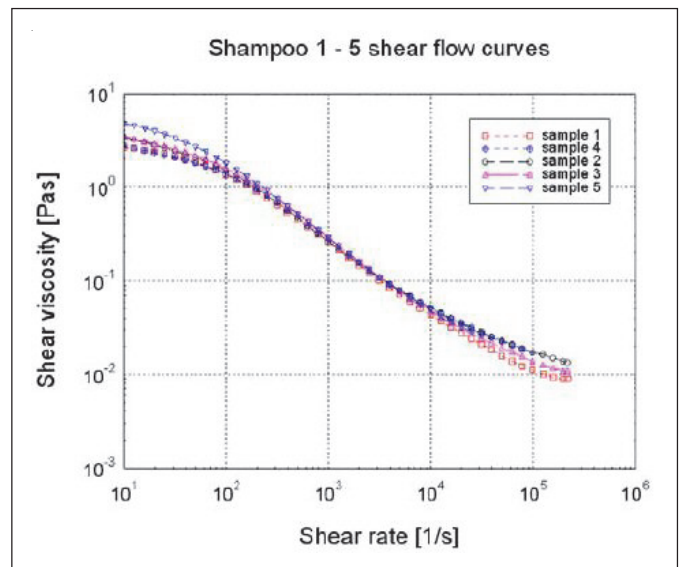


Fig. 4: Shear viscosity curves of shampoos 1-5.

The graph of the extensional flow curves (see Figure 6) shows that the extensional viscosities of samples 1 and 2 (which performed well in the high speed filling line) are clearly lower than those of samples 3 and 5 (which did not perform well in the high speed filling line). The lower extensional viscosity leads to a higher strain rate and shorter break-up time (filament life time) in the CaBER experiment and in the filling equipment.

Conclusions

The HAAKE CaBER 1 extensional rheometer allows for an easy quick determination of the extensional flow properties of low to medium viscous fluids. In the presented case it was possible to distinguish between different shampoos and of predicting filament lifetimes for production and quality control. Shampoos 3 - 5 will need to be reformulated to solve the serious filling problems. In this way it is possible to optimize the quality of the shampoos and the production process.

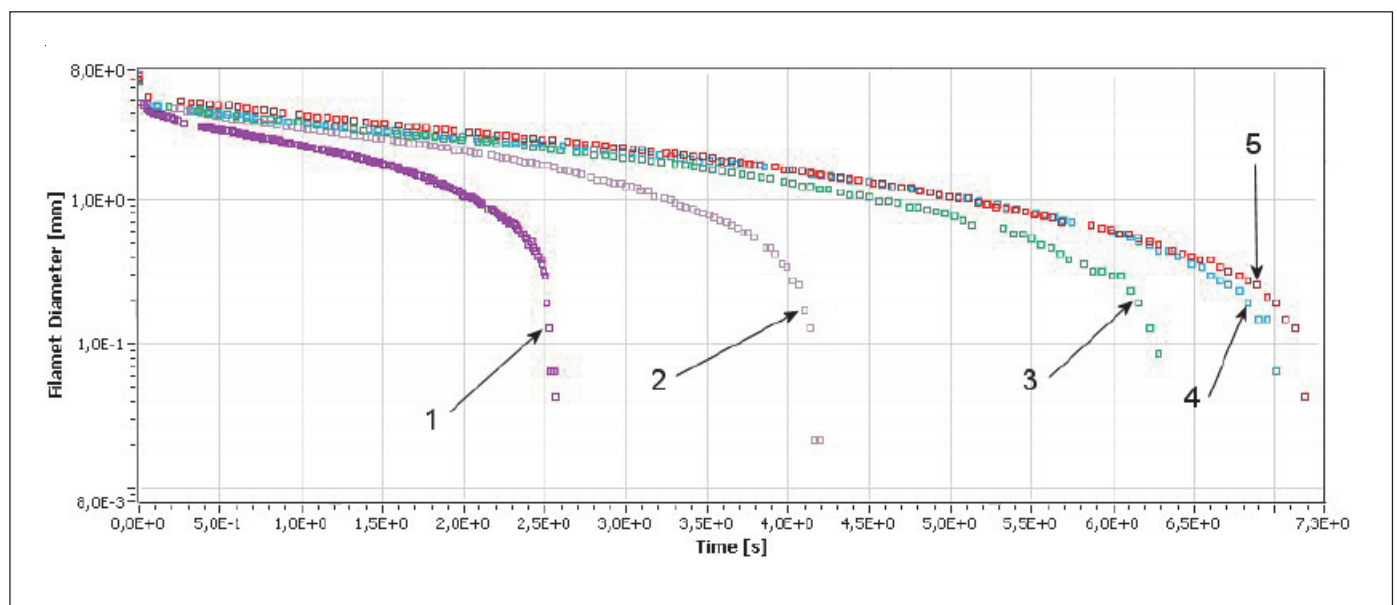


Fig. 5: Filament diameter decay of shampoos in the CaBER experiment.

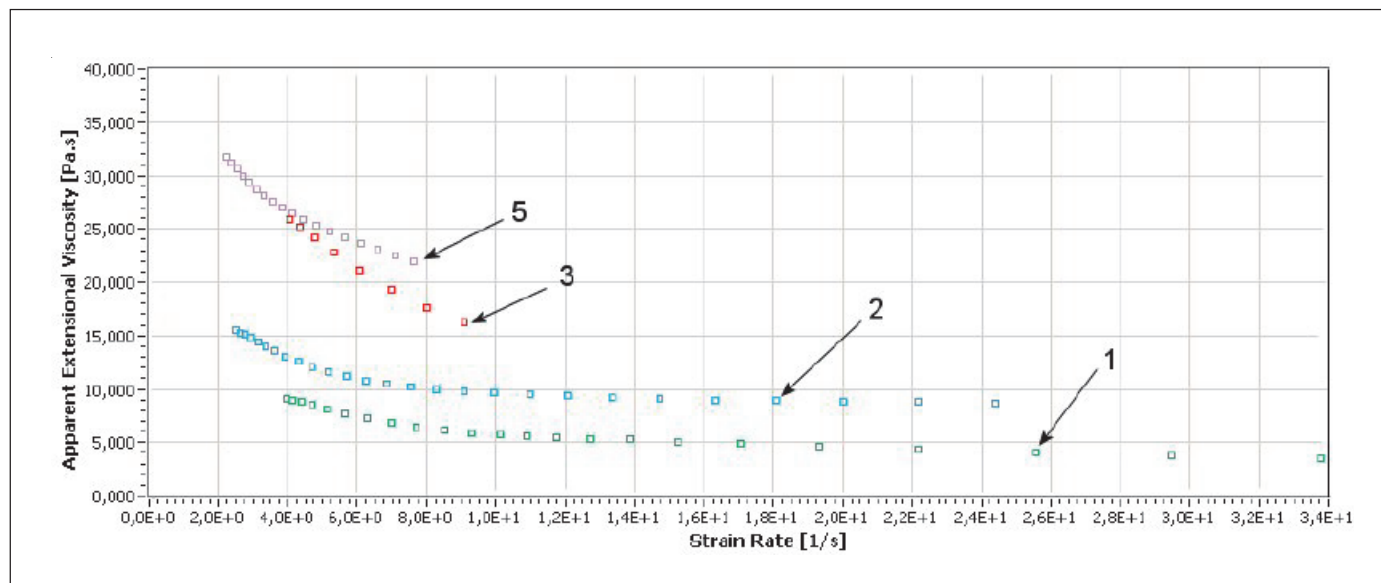


Fig. 6: Extensional flow curves of shampoos 1-5.

References

- [1] <http://www.hairshampoo.com>
- [2] Laba D. (ed.): Rheological properties of cosmetics and toiletries - Cosmetic science and technology series vol. 13. Marcel Dekker, New York (1993)
- [2] Henning T., Milbradt R., Miller D.: Stabilising special-effect particles, Cossma 3 (2003), 48-49.

Find out more at thermofisher.com/rheometers

ThermoFisher
SCIENTIFIC

Classification of herbs by FT-NIR Spectroscopy using the Thermo Scientific Antaris II Analyzer

Authors

Martin Hollein, Nicolet CZ s.r.o.
Prague, Czech Republic

Todd Strother
Thermo Fisher Scientific
Madison, WI, USA

Key Words

Antaris, TQ Analyst, closed sample cup, cosmetics, discriminant analysis, FT-NIR, herbs, pharmaceuticals, sample cup spinner

Introduction

Vibrational techniques like Fourier transform near-infrared (FT-NIR) spectroscopy are well-suited for raw material identification. This is because FT-NIR is sensitive to the characteristic molecular vibrations that occur for specific compounds. Because of this ability to detect molecular vibrations, NIR spectrometers are widely used in the pharmaceutical industry for classifying pure chemicals or their mixtures. Compounds usually contain highly absorbing functional groups (alkyls, phenyls, amines, thiols, hydroxyls, acids, esters, etc.) which allows for unambiguous identification within seconds. The Thermo Scientific™ Antaris™ line of FT-NIR spectrometers (Figure 1) is ideally suited for raw material identification of pure chemicals as well as complex biological samples used in pharmaceutical, nutraceutical and related industries.



Figure 1: The Antaris II FT-NIR analyzer showing different available detection options

While herbs and their extracts are often used in cosmetics and nutraceuticals, they additionally find use as raw materials in classic pharmaceutical industries. Often, these herbal active ingredients or their intermediates are isolated from raw materials using extraction or chromatographic techniques. Herbs used in pharmaceuticals must be treated like any another raw material in the manufacturing facility and must fulfill all of the regulatory demands as any other “chemical” raw material.

Researchers at IREL, spol. s.r.o. (Brno, Czech Republic) explored FT-NIR spectroscopy as a means to rapidly identify herbs used to produce extracts found in nutraceuticals, cosmetics and pharmaceuticals. Their biological origin means that many herbs contain similar components, like cellulose, proteins and sugars, which tend to result in similar spectra. The purpose of this application note is to demonstrate that complex herbal materials can be correctly classified using FT-NIR spectroscopy much more rapidly than conventional techniques.

Experimental

The standard herbs used to develop the analysis method were supplied by IREL, spol s.r.o. and used directly to produce the fluid extracts – no additional grinding or sieving was performed. Particle size varied substantially among the samples. Leaves were typically thin and as large as 6 x 6 mm. Roots, galls and orange peels were crushed to maximum particle sizes of 10 x 10 x 5 mm. The list and description of the 14 herbs used in the data collection is summarized in Table 1.

Herbal Name	Scientific Names
Agrimony – top	Agrimonia eupatoria L.
Buckbean – leaf	Menyanthes trifoliata L.
Calamus – root	Acorus calamus L.
Camomile – flowers	Matricaria recutita
Gentian – root	Gentiana lutea L.
Hot pepper – powdered fruit	Capsicum sp.
Myrrh – powdered gum resin	Commiphora molmol E.
Oak Apple – crushed gall	Diplolepis quercus-folii
Orange Peel	Citrus Aurantium L.
Sage – top	Salvia officinalis L.
Valerian – root	Valeriana officinalis L.
Walnut – leaf	Juglans regia L.
Witch Hazel – leaf	Hamamelis virginiana L.
Wormwood – top	Artemisia absinthium L.

Table 1: List of herbal samples used in analysis

Three or four samples of each herb were scanned with an Antaris II FT-NIR system in the range between 10,000 and 4,000 cm^{-1} . The materials were placed in a closed rotating sample cup with a 30 mm window over the integrating sphere (Figure 2).



Figure 2: Antaris II analyzer with the closed sample cup and spinner

Spectra and other calibrations data were collected and archived using the validated Thermo Scientific™ RESULT software. Each sample spectra was the result of 50 scans using 4 cm^{-1} resolution. These parameters allowed the material to be scanned through two full rotations of the sample cup in less than one minute.

The resulting spectra were evaluated with Thermo Scientific™ TQ Analyst software using a Discriminant Analysis algorithm in order to classify the samples. Multiplicative Signal Correction (MSC) pathlength type was chosen because it is designed for analysis of samples, such as solids, where it is difficult to obtain an independent pathlength measurement. Because of light scattering, pathlength is then treated as a multiplicative contribution to the spectral signal. The software applies the same function to the standards and the unknown samples. The raw spectra in the range between 9,900 and 4,100 cm^{-1} were used for the calibration algorithm. A linear removed baseline correction was used but no other mathematical smoothing or derivative functions were applied.

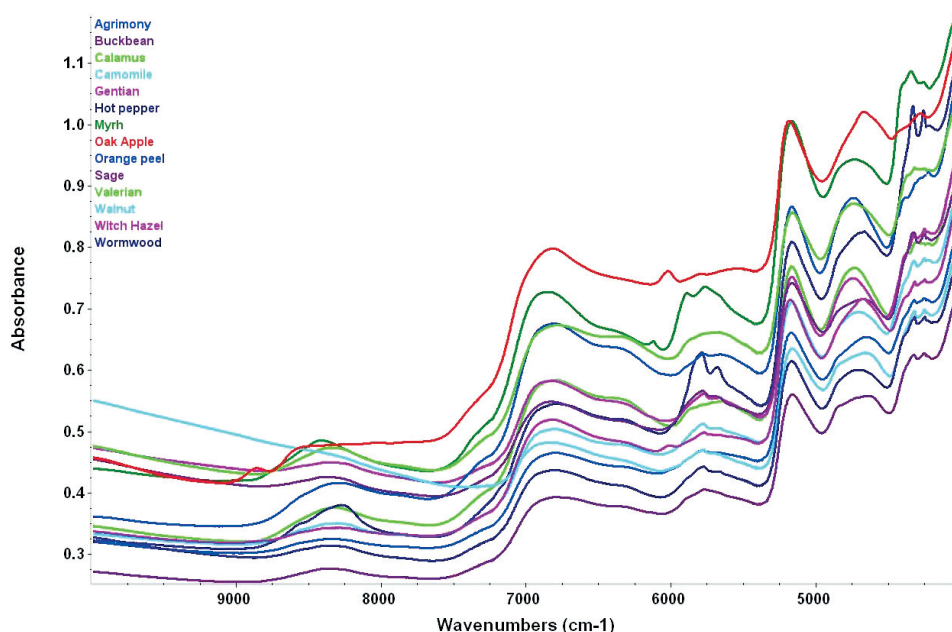


Figure 3: Representative spectra of the 14 samples used in the analysis.

Results and discussion

Figure 3 is the plot of average diffuse reflection spectra of the 14 herbs. The samples show substantial spectral variation that can be exploited for building the classification model. Using Discriminant Analysis as the chemometric method 99.5% of the spectral variability was described with five principal components. Principal components are orthogonal vectors that describe spectral variation in a set of standards. The first principal component will account for most of the spectral variation and subsequent components account for the remaining variation. Generally, the fewer components required to describe the total variation results in a more robust method.

This method correctly classified all of the standards as well as randomly chosen validation spectra from each class. One means of determining the quality of a chemometric method is through Mahalanobis distance analysis. The Mahalanobis distance can be described as the spectral distance a particular sample is from the “center of mass” of the group. For samples that are spectrally similar to a particular class or group, the Mahalanobis distances will be

relatively small. Samples that are spectrally very different than the class will have high Mahalanobis distances. For the samples under consideration, the Mahalanobis distances of the nearest incorrect class were at least twice the distance to the correct class; indicating good spectral separation and accurate classification. The distances of the nearest and next nearest classes are shown in Table 2.

Principal Component Scores plots show spectra variation for samples in two dimensions. Figure 4 is a Principal Component Scores plot that shows clusters of different classes described by the first two principal components. Most of the classes are tightly clustered with standards that are near each other. Extremely homogeneous samples were most tightly clustered (i.e., powdered hot pepper). Those that have dispersed clusters are classes with irregular shaped particles or heterogeneous samples (i.e., walnut leaf, oak apple-crushed gall). The Principal Component Scores plot shows no overlap between the different classes when viewed in multidimensional space indicating that the samples can be successfully and easily classified.

Class ID	Distance	Next Distance	Next Class
Agrimony	0.5	4.0	Camomile
Agrimony	0.7	3.6	Camomile
Agrimony	1.0	3.5	Buckbean
Buckbean	0.2	3.3	Camomile
Buckbean	0.2	3.3	Camomile
Buckbean	0.4	3.1	Camomile
Calamus	0.7	2.8	Orange Peel
Calamus	0.7	3.7	Orange Peel
Calamus	0.4	3.0	Orange Peel
Camomile	1.0	2.1	Wormwood
Camomile	0.9	2.1	Wormwood
Camomile	0.6	2.2	Wormwood
Gentian	0.2	5.0	Calamust
Gentian	0.4	5.0	Calamust
Gentian	0.4	4.8	Calamust
Hot Pepper	0.1	13.2	Wormwood
Hot Pepper	0.1	13.3	Wormwood
Hot Pepper	0.1	13.2	Wormwood
Myrrh	0.3	7.4	Sage
Myrrh	0.4	7.3	Sage
Myrrh	0.5	7.3	Wormwood
Oak Apple	0.5	5.5	Witch Hazel
Oak Apple	0.9	5.0	Witch Hazel

Class ID	Distance	Next Distance	Next Class
Oak Apple	0.8	6.2	Witch Hazel
Oak Apple	0.9	6.4	Witch Hazel
Orange Peel	1.3	3.1	Calamus
Orange Peel	0.8	2.8	Calamus
Orange Peel	0.7	3.6	Calamus
Orange Peel	1.2	3.6	Calamus
Sage	1.0	4.6	Wormwood
Sage	1.0	6.2	Wormwood
Sage	0.8	5.0	Wormwood
Valerian	1.1	7.0	Gentian
Valerian	0.9	6.6	Gentian
Valerian	0.7	6.6	Gentian
Walnut	1.6	10.6	Agrimony
Walnut	2.0	13.0	Agrimony
Walnut	1.1	10.2	Agrimony
Walnut	1.7	11.3	Agrimony
Witch Hazel	0.8	5.9	Agrimony
Witch Hazel	0.9	5.7	Oak-Apple
Witch Hazel	0.6	5.5	Oak-Apple
Wormwood	0.6	2.2	Camomile
Wormwood	0.7	1.8	Camomile
Wormwood	0.2	2.1	Camomile

Table 2: Chart showing the Mahalanobis distance of each sample to its identified class. The distance to the next nearest class is included as a quantitative indication of how close the samples are to an incorrect class. Lower numbers indicate spectral similarity to a class, higher numbers indicate spectral dissimilarity. All of the samples were correctly identified.

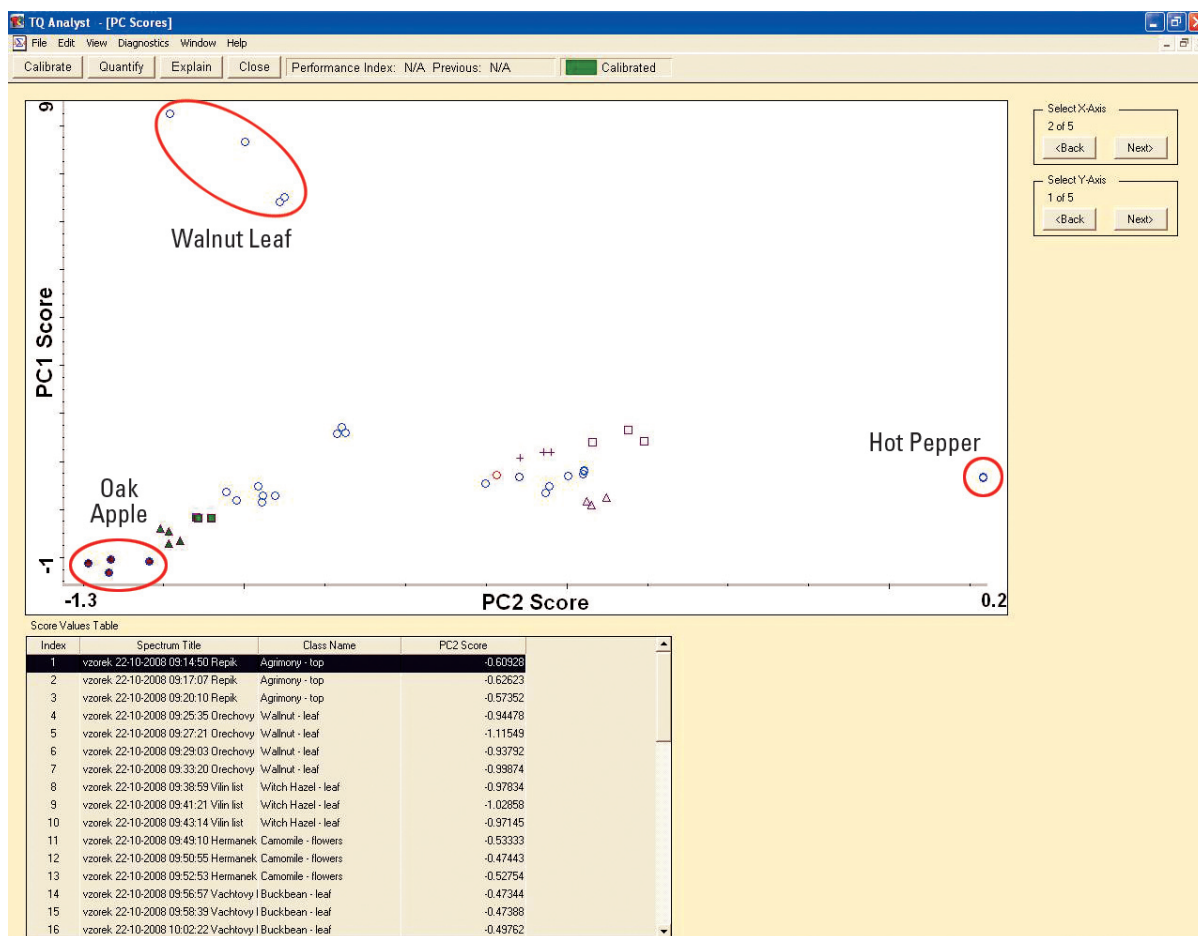


Figure 4: Principal components scores plots showing the class clustering as a function of the first and second principal component. Heterogeneous samples tended to have widely scattered clusters (Walnut Leaf, Oak Apple), while homogeneous samples were tightly clustered (Hot Pepper). There were well defined and no overlapping clusters for the classes when viewed in 5 dimensional principal component space.

Conclusion

The Antaris II FT-NIR analyzer offers an excellent alternative to traditional identification and classification methods (i.e., descriptive morphology, TLC and HPLC chromatography) of herbal extracts used in nutraceuticals, cosmetics and pharmaceuticals. There is no need for additional grinding, cutting, sieving or other preparation of the samples. This results in a great reduction in time and

labor required to properly classify incoming raw materials used in these industries. Additionally, the sample cup spinner accessory with the closed sample cups allows for the reproducible collection of spectra from heterogeneous samples. The Discriminant Analysis method developed here for analysis of the 14 herbs is shown to be robust and reliable while providing answers within seconds.

Find out more at www.thermofisher.com

ThermoFisher
SCIENTIFIC

Monitoring emulsions morphology under shear via simultaneous rheometry and in-situ FT-IR spectroscopy

Authors

Kiyoji Sugimoto¹, Fritz Soergel², and Manfred Feustel³

¹Thermo Fisher Scientific, Yokohama, Japan

²Thermo Fisher Scientific, Karlsruhe, Germany

³Resultec analytic equipment, Illerkirchberg, Germany

Introduction

Emulsions are of wide interest in the food, pharmaceutical, healthcare and cosmetic industries. They typically consist of at least two liquid phases, surfactant agents and stabilizers. Emulsions exhibit complex rheology, making it difficult to understand flow phenomena on a microscopic level.

A common technique utilized to analyze emulsions under shear deformation is light microscopy. However, emulsions showing droplet distributions with droplets on the submicron scale cannot be visualized using light microscopy because of given resolution constraints. Other limiting factors of light microscopy arise when the concentration of droplets with equal size is high or the refractive indices of the two phases are too similar.

In such cases, the Thermo Scientific™ HAAKE™ MARS™ rheometer equipped with the Rheonaut module and a FT-IR spectrometer provides simultaneous rheometry and in-situ FT-IR spectroscopy under shear deformation and offers a versatile tool for efficient and comprehensive emulsion research and stability testing. Simultaneous rheometry and FT-IR spectroscopy proves to be a useful tool in understanding the microscopic state of droplets in concentrated emulsions.

In this contribution, we want to present some results on the dynamics of molecular organization of an emulsion under shear.

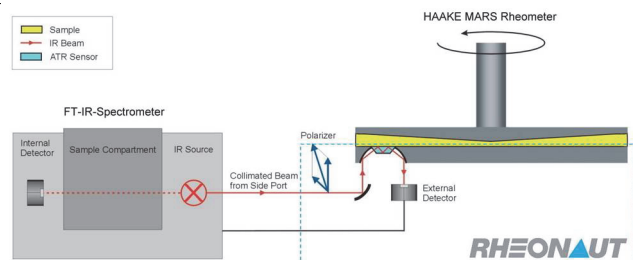


Fig. 1: Schematic diagram of coupling an FT-IR spectrometer to the HAAKE MARS rheometer.



Fig. 1: The HAAKE MARS rheometer with Rheonaut module and Nicolet iS 10 FT-IR spectrometer.

Materials

For this study, as model substances, three commercially available hand cream emulsions with high volume fractions of oil in water containing submicron droplets were supplied by a manufacturer of cosmetics. The samples varied with respect to their hydrocarbon composition only. No further sample preparation was required.

Methods

The patented* Rheonaut module couples a standard FT-IR spectrometer with side port (here: Thermo Scientific™ Nicolet™ iS™ 10 FT-IR spectrometer) to the HAAKE MARS rheometer.

The lower plate of the rheometer is temperature controlled (Peltier or electrical) and features a monolithic diamond element that serves as the ATR (attenuated total reflection) sensor, offering a single internal reflection. Compared to

*Resultec Analytic Equipment: DE 10140711, EP 02762251, US 6988393, JP 4028484

standard infrared transmission spectroscopy or specular reflection spectroscopy techniques, the sample thickness can thus be adjusted to the rheological needs and is independent from the infrared spectroscopy requirements.

The operation is managed by the Thermo Scientific™ HAAKE™ RheoWin™ software providing full control over temperature settings, horizontal positioning of the lower plate, and the communication with the FT-IR spectrometer software for synchronous data acquisition.

Steady shear flow experiments were carried out using a cone/plate measuring geometry with 20 mm diameter and a cone angle of 2°. Gap setting was 0.1 mm. All samples were tested in CR (controlled shear rate) mode from 0.5

up to 500 s⁻¹. The temperature was set to 25.0 ± 0.1 °C. The infrared spectral range was 400 cm⁻¹ to 4000 cm⁻¹ with a spectral resolution of 4 cm⁻¹. Each spectrum consists of 8 co-added scans.

A complete data set was produced for each sample, consisting of 18 rheological data points and 18 related (simultaneously collected) FT-IR spectra.

Results

Figure 3 displays the dynamic shear viscosity plotted against shear rate for the three samples #1, #2, and #3. As typical for highly concentrated emulsions, the materials show a decreasing viscosity with increasing shear rate (shear thinning or pseudoplastic).

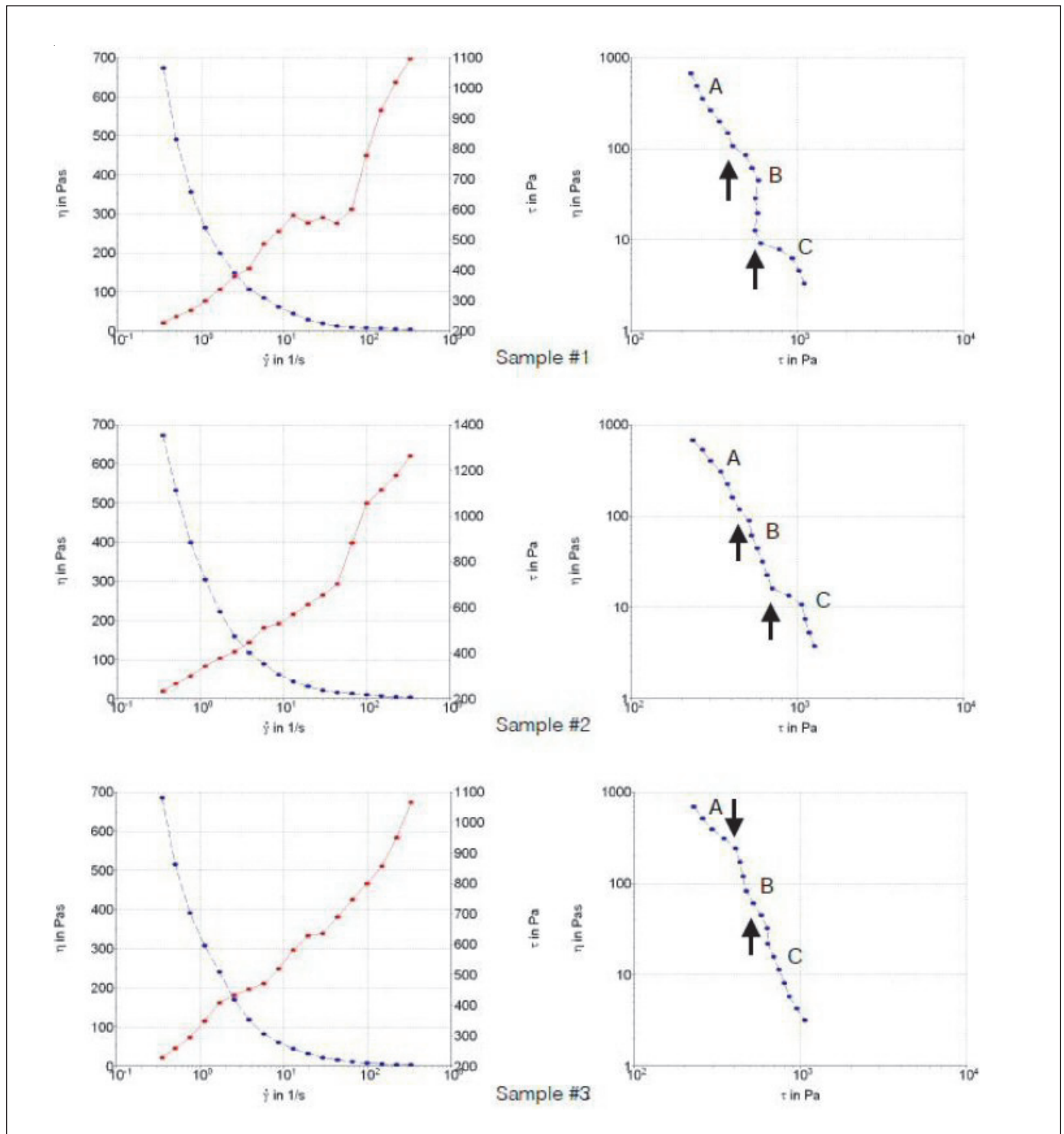


Fig. 3: Left column: Viscosity η (blue graph) and stress τ (red graph) plotted against shear rate. Right column: Viscosity η (log scale) plotted against stress τ .

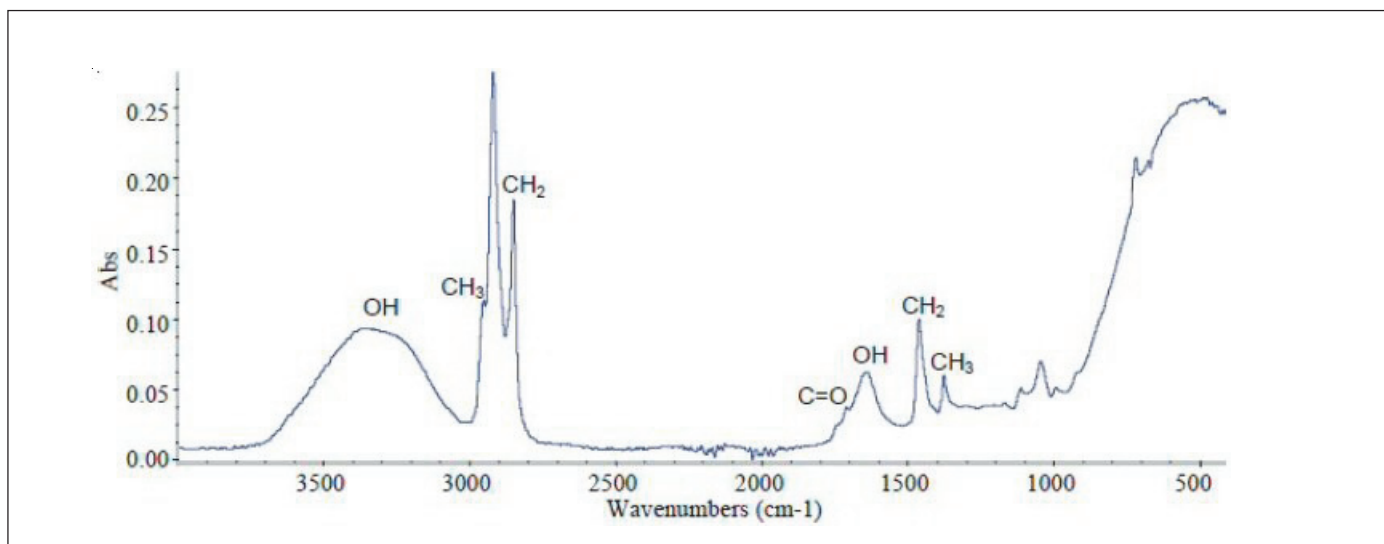


Fig. 4: A typical FT-IR absorbance spectrum with band assignments of the investigated samples.

A closer look, however, reveals a step-like shear thinning behavior as can be seen in the right graphs of figure 3 which display the viscosity plotted double-logarithmically against shear stress.

Such a viscosity behavior has been investigated amongst others by Saiki et al. [1]. Based on detailed rheological experiments, the proposed figurative model is a droplet distribution profile which changes with the applied stress. Whereas at very low shear the droplets are distributed homogeneously, ambiguous layers (or clusters) of droplets are formed at moderate shear causing slight segregation in droplet population and at higher shear discrete layers are formed. Another approach [2] proposes a figurative model showing a droplet deformation and stretching by the applied shear, leading to droplet rupturing and recombination through coalescence at higher shear stresses.

Simultaneously applied FT-IR spectroscopy enables a more sophisticated molecular insight and deeper understanding. Figure 4 displays a typical FT-IR sample spectrum. The broad absorption band at 3354 cm^{-1} relates to the aqueous phase of the sample whereas the band at 2922 cm^{-1} relates to the organic phase.

The sample changes with shear get easily traceable by calculating the absorption ratio ($3354\text{ cm}^{-1}/2922\text{ cm}^{-1}$) from each spectrum and plotting the results against the experimental procedure (figure 5).

The change of the infrared absorption ratios in figure 5 reveals a concentration gradient within the samples. Close to the ATR sensor are sample layers at which the organic phase is enriched in relation to the aqueous phase.

As the experiment goes on, the enrichments dissolve again. Because the ATR sensor area dimensions are several orders of magnitude larger than the submicron droplets of the organic phase, neither droplet deformation and stretching nor coalescence is an object since they do not evoke a concentration gradient within a sample.

The shear thinning behavior of the investigated emulsion samples is initially controlled by perturbation and breakdown of complex droplet structures which lead to the formation of droplet layers causing flatter shear viscosity curve regions. With further increasing shear rates, however, a self-healing process is observed. The droplet structure is rearranged and hence the layers are dissolved, as the FT-IR spectra show.

Conclusion

Rheometry and FT-IR spectroscopy have been applied simultaneously on model emulsions (3 commercially available hand creams) to study the structure development of emulsions under shear stress.

The results prove an ability of the investigated emulsions to repair the damage caused by mechanical impacts over time.

The Rheonaut offers a new approach to rheology by providing molecular insight and can thus reveal information about molecular organization and dynamics under deformational flow.

The exact knowledge of the interacting fundamental structuring mechanisms creates the basis for an optimized tuning of technical, process engineering, and material parameters with respect to a functionally optimized structuring of emulsion systems.

References

- [1] Saiki, Y. and Prestidge, C.A., Korea-Australia Rheol. J. 17 (2005), 191-198
- [2] Mason, T.G., Curr. Opin. Colloid Interface Sci. 4 (1999), 231-238

Presented at the 6th International Symposium on Food Rheology and Structure, April 10-13, 2012, Zurich, Switzerland

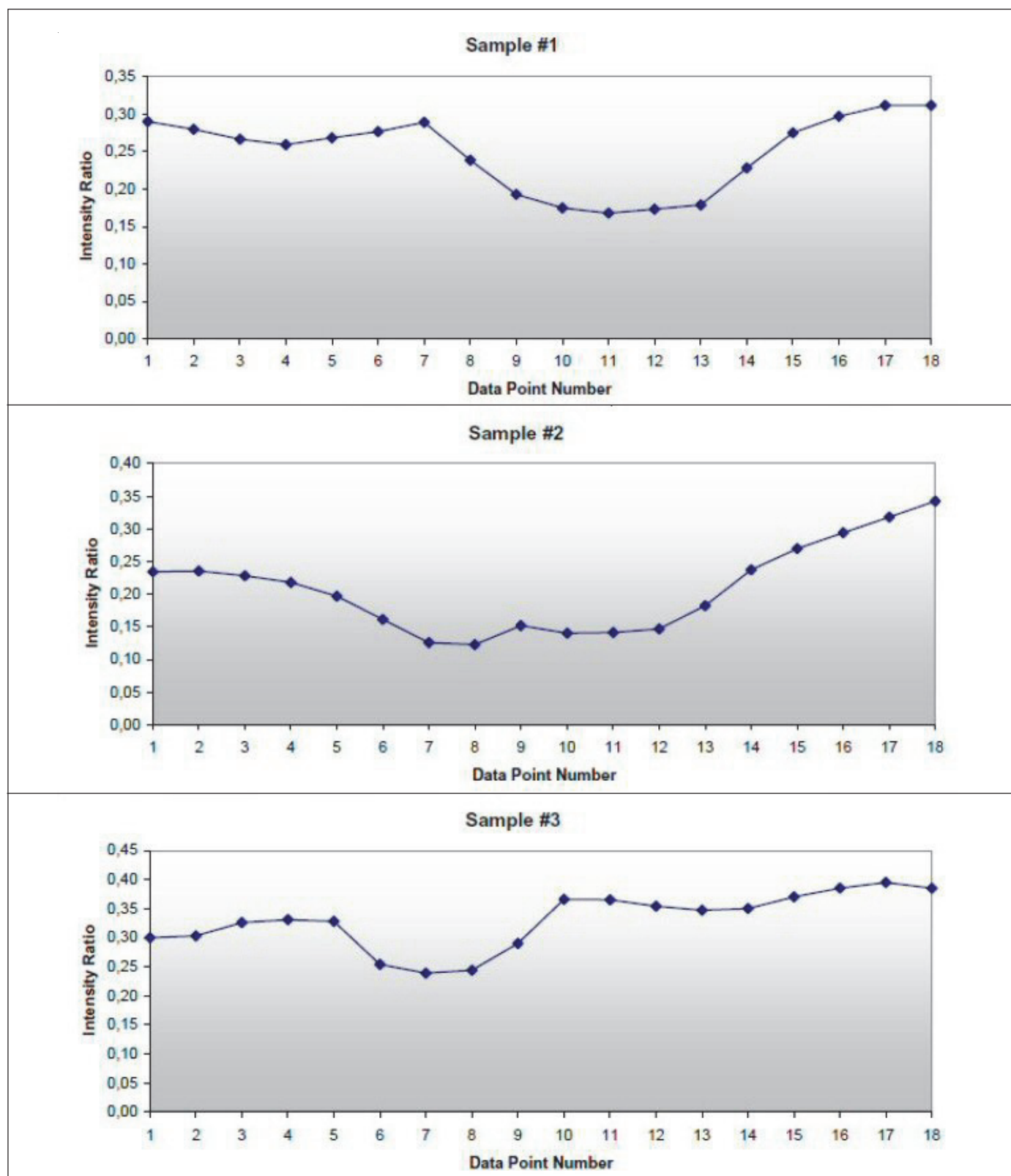


Fig. 5: Absorption ratio ($3354\text{ cm}^{-1}/2922\text{ cm}^{-1}$) from each FT-IR spectrum plotted against the data point number.

Find out more at thermofisher.com/rheometers

ThermoFisher
SCIENTIFIC

Rheology-Raman Spectroscopy: Tracking emulsion stability with the combination of a rheometer and Raman spectrometer

Authors

Jan P. Plog¹ and Matthew Meyer²

¹Thermo Fisher Scientific, Karlsruhe, Germany

²Thermo Fisher Scientific, Madison, USA

Key words

Rheology, Raman spectroscopy, Emulsions, Shelf life, Combined methods

Introduction

As the stress-strain response of complex fluids is closely linked to changes in physical or chemical structure within the material, rheology can be most useful when combined with simultaneous measurement of physical or chemical properties affecting flow.

Chemical information including molecular conformation, bond formation or scission, and chemical composition is also critically relevant to rheological measurements. Vibrational spectroscopic tools such as Raman spectroscopy have proven to be powerful noninvasive techniques to probe chemical information of interest in a variety of soft matter systems including emulsions [1].

The benefit of simultaneous measurements is clear: many soft materials are sensitive to temperature and flow history, so simultaneous measurements minimize experimental variation.

In this application note, we present results obtained on a cosmetic emulsion in cooperation with NIST published previously [2].

The results shown can be obtained with the brand new combination of a Thermo Scientific™ HAAKE™ MARS™ rheometer with a Thermo Scientific™ iXR Raman spectrometer (Thermo Scientific™ HAAKE MARSxR RheoRaman System) as shown in Fig. 1.

Result and discussion

The experimental setup shown in Fig. 1 represents a novel integration of commercial instrumentation: a Raman spectrometer (Thermo Scientific iXR Raman) and rotational rheometer (HAAKE MARS) are coupled through an optically transparent base modified from the Thermo Scientific™ RheoScope Module.



Fig. 1: The Thermo Scientific HAAKE MARSxR RheoRaman system.

The cosmetic emulsion tested consists of oil droplets suspended in water and is stabilized by a mixture of surfactants. The Raman spectra of the emulsion over the spectral range at 25 °C is shown in Fig. 2a. The broad peak in the range of 200 cm⁻¹ to 600 cm⁻¹ is attributed to the fused silica window between the objective and the sample. Additionally, a small sharp band at 2330 cm⁻¹ is due to ambient nitrogen. A number of peaks are observed in the fingerprint region of 650 cm⁻¹ to 1600 cm⁻¹ and are magnified in Fig. 2b. Although a complete chemical component analysis based on the measured spectra is outside the scope of this application note, the sharp peaks in the fingerprint region appear at positions attributed to the vibrational bonds of alkyl groups C_nH_{2n+1}: the C-C symmetric and asymmetric stretch peaks at 1063 cm⁻¹ and 1130 cm⁻¹ respectively, the CH₂ twist mode at 1296 cm⁻¹, and multiple modes associated with CH₂ bending motion at 1418 cm⁻¹, 1441 cm⁻¹, and 1464 cm⁻¹.

These alkyl group modes are present due to the alkyl chains present on the stabilizers and fatty acids comprising the majority of the coconut and almond oils in the emulsion. The broad distribution of Raman bands in the range of 750 cm^{-1} to 950 cm^{-1} is common for C-O-C stretch modes expected for the polyethylene oxide groups present in polysorbate CH_2 rocking modes for fatty acids and alcohols [3]. The presence of methyl CH_2 groups is further evidenced by the presence of peaks in the 2600 cm^{-1} to 3000 cm^{-1} region (shown in greater detail in Fig. 2c) attributed to CH_2 and CH_3 stretching modes.

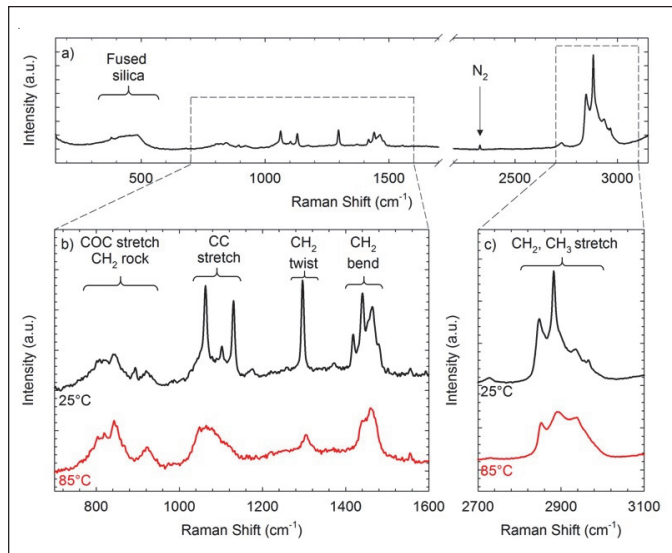


Fig. 2: (a) Raman spectra of the emulsion at room temperature over the instrument range. (b) Raman spectra of the emulsion in the range of (700 to 1600) cm^{-1} at temperatures indicated in the figure. (c) The same spectra collected in (b) in the (2700 to 3100) cm^{-1} region. Note that the intensity scaling varies from (b) to (c).

Upon heating, the sharp peaks due to the C-C stretch, CH_2 twist, and CH_2 bend modes decrease in intensity relative to broader peaks in the spectra as shown in Fig. 2b. A similar loss of intensity of the sharp peak at 2883 cm^{-1} in Fig. 2c is evident at the higher temperature. The loss of intensity in these peaks corresponds to increasing conformational disorder along the alkyl chains present in the stabilizer, fatty acid, and fatty alcohol chains due to melting.

Quantitative measurement of alkyl chain measurement can be obtained by analysis of the peaks associated with the CH_2 twisting modes [4]. Our analysis of the spectra in the CH_2 twist region follows a similar protocol used to quantify *consecutive trans* and amorphous conformers in alkanes and polyethylenes [5]. The Raman spectra are fit using two Lorentzian peaks: a narrow peak of approximately 2 cm^{-1} FWHM centered at 1296 cm^{-1} and a broader peak of approximately 13 cm^{-1} FWHM at 1303 cm^{-1} . These fits are used to calculate the integrated area I of each peak. The total area under the curves in the CH_2 twist region $I_{1296} + I_{1303}$ is invariant with respect to chain disorder, which provides a method to normalize the spectra. The area of the peak at 1296 cm^{-1} normalized by the total area

$$I' = \frac{I_{1296}}{I_{1296} + I_{1303}} \quad (1)$$

then quantifies the mass fraction of chains with more than four consecutive trans sequences along the chain. The value of I' quantifies the mass fraction of ordered chains.

Simultaneous Raman and viscosity measurements of the emulsion are shown in Fig. 3 for the temperature ramp from 25 $^{\circ}\text{C}$ to 90 $^{\circ}\text{C}$ at a rate of 1 $^{\circ}\text{C}/\text{min}$. The viscosity is measured at a steady shear rate of 30 s^{-1} and a gap thickness of 200 μm . Lower shear rates lead to shear localization in a thin fluid layer between the rotor and the droplet phase, which is confirmed via polarized optical imaging of immobile droplets in the bulk (however, this phenomenon is beyond the scope of this manuscript.) The viscosity decreases with increasing temperature until approximately 50 $^{\circ}\text{C}$, at which point the viscosity sharply decreases.

The temperature range of 45 $^{\circ}\text{C}$ to 55 $^{\circ}\text{C}$ where viscosity and *consecutive trans* fraction exhibit a strong temperature dependence, correlates well with the melting temperatures of stabilizers in the emulsion including cetyl alcohol and stearylalkonium chloride. These simultaneous measurements allow for clear correlation of steady shear viscosity with conformational information.

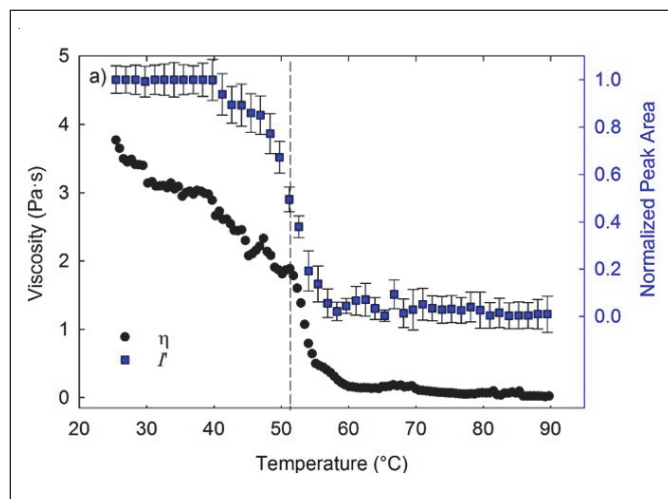


Fig. 3: Viscosity and normalized peak area I' as a function of temperature for the emulsion.

Summary

With the Thermo Scientific HAAKE MARSxR RheoRaman System, simultaneous measurements of rheological properties and Raman-active molecular vibrations are possible. The emulsion example shown in this work, highlights the applicability of the MARSxR to characterize structural and conformational changes directly related to the rheological response of the material. Since all measurements are performed simultaneously, experimental conditions such as temperature and flow history are identical for Raman and rheology. In addition, the laser excitation and collection path can be equipped with optical elements for polarized Raman measurements. Based on the possibilities for direct correlation between chemical, structural, and mechanical properties, we expect the MARSxR to be critically relevant to both academic and industrial interests.

References

- [1] M. Amer, Raman spectroscopy for soft matter applications (John Wiley & Sons, 2009).
- [2] A. P. Kotula et. al., Review of Scientific Instruments 87, 105105 (2016).
- [3] J. De Gelder, K. De Gussem, P. Vandenabeele and L. Moens, J. Raman Spectrosc. 38, (2007).
- [4] K. G. Brown, E. Bicknell-Brown and M. Ladjadj, J. Phys. Chem. 91, (1987).
- [5] K. B. Migler, A. P. Kotula and A. R. Hight Walker, Macromolecules 48, (2015).

Find out more at thermofisher.com/msr

ThermoFisher
SCIENTIFIC

APPLICATION NOTE

Stability of cosmetic emulsions quantified with rheology and simultaneous DEA

Author

Klaus Oldörp
Thermo Fisher Scientific, Karlsruhe, Germany

Key words

Emulsions, stability, rheology, simultaneous DEA

Introduction

Cosmetic emulsions have to meet consumer demands from many perspectives. They should have the desired effect on the skin, they should have a nice look and feel and they should not change their texture over several months. All these properties are closely related to the long-term stability of an emulsion. Only from a stable emulsion we can expect the active ingredients to stay homogeneously distributed, an unchanged look and feel and texture.

The Thermo Scientific™ HAAKE™ MARSTM rheometer is a versatile universal rheometer, which allows various combinations with other analytical techniques. For the verification of an emulsion's stability, the integration of a dielectric analysis DEA has been selected.

While the HAAKE MARS can measure the mechanical properties of an emulsion, the DEA can give information about the microscopic conditions inside the emulsion under precisely defined stresses, deformations and temperatures set by the rheometer.

Regarded in a simplified way, a DEA applies an oscillating voltage to a sample between 2 electrodes and measures the resulting current due to the mobility of charged molecules (ions) in the electrical field. This mobility is influenced by the resistivity of the sample matrix, which is correlated to the viscosity or modulus of the sample. The results of a DEA measurement can be expressed with the so-called ion viscosity, which is the reciprocal ion mobility or reciprocal conductivity of the sample. In other words, the ion viscosity increases when the ion mobility is decreases.

Samples

Two different batches of a skin cream have been selected for testing due to their difference in appearance.



Fig. 1: A lower measuring plate with Mini IDEX comb sensor.

While one batch represented the usual quality of the cream with a matt white surface and a rather “solid” appearance the, other had a significantly glossier surface, softer edges and also felt softer on the skin.

Test conditions

The tests have been performed using a 20 mm plate/plate geometry with a gap of 1 mm. Sample loading has been done avoiding unnecessary shearing and with reduced lift speed while closing the gap.

A lower measuring plate (TMP) with a DEA comb sensor [1] has been used to collect the ion viscosity at different frequencies (Fig. 1). The sensor was connected to a DEA 288 Epsilon (NETZSCH-Gerätebau, Selb, Germany). During the measurements, the NETZSCH Proteus® software was triggered by the Thermo Scientific™ HAAKE™ RheoWin™ software at the start of the rheological measurement to guarantee simultaneous data acquisition.

Since the DEA sensor consists of a pair of interdigitated electrodes, the DEA measurement is independent of the rheometer's measuring gap, as long as the gap size is bigger than the distance between the 2 electrodes.

With this setup, an amplitude sweep and a temperature run have been done on both samples. The amplitude sweep was performed at 20 °C and using the controlled deformation (CD) mode, to have a better control of the measurement conditions.

To characterise the temperature dependant behaviour, fresh samples have been heated up from 0 °C to 40 °C with a heating rate of 1 K/min.

Results and Discussion

The appearance of a cream sold in a pot strongly depends on to what extent it flows under its own weight or not. Another part of the consumer perception is related to the cream's handling properties. In other words, how does the cream feel, when taking a bit out of the pot and rubbing it onto the skin?

Since these properties are related to the force required to make the cream yield, the results of the amplitude sweep have been plotted as a function of the stress applied (Fig. 2), although the measurement has been done with deformation control (CD mode).

The end of the linear viscoelastic range (LVR) has been calculated based on the storage modulus (G') and a 10 % deviation from the plateau value. Between the softer (less stable, open symbols) and the harder (stable, filled symbols) cream lies a factor of about 8 in stress.

Regarding the results from the DEA (Fig. 3), we see an increase of the ion viscosity at higher times, which correspond to higher stresses. The less stable cream shows the earlier increase after 4.8 min, when the sample was exposed to a stress of 4.2 Pa, whereas the stable sample shows this increase after 7.2 min or at 40 Pa (stress/time correlation not shown in Fig. 2).

It is interesting to see, that in both cases the onset of the ion viscosity increase occurs at stresses about 4 times higher than the stresses for the end of the LVR calculated from the rheological results. Similar to the rheological results, the onset of the increase differs by a factor of almost 10.

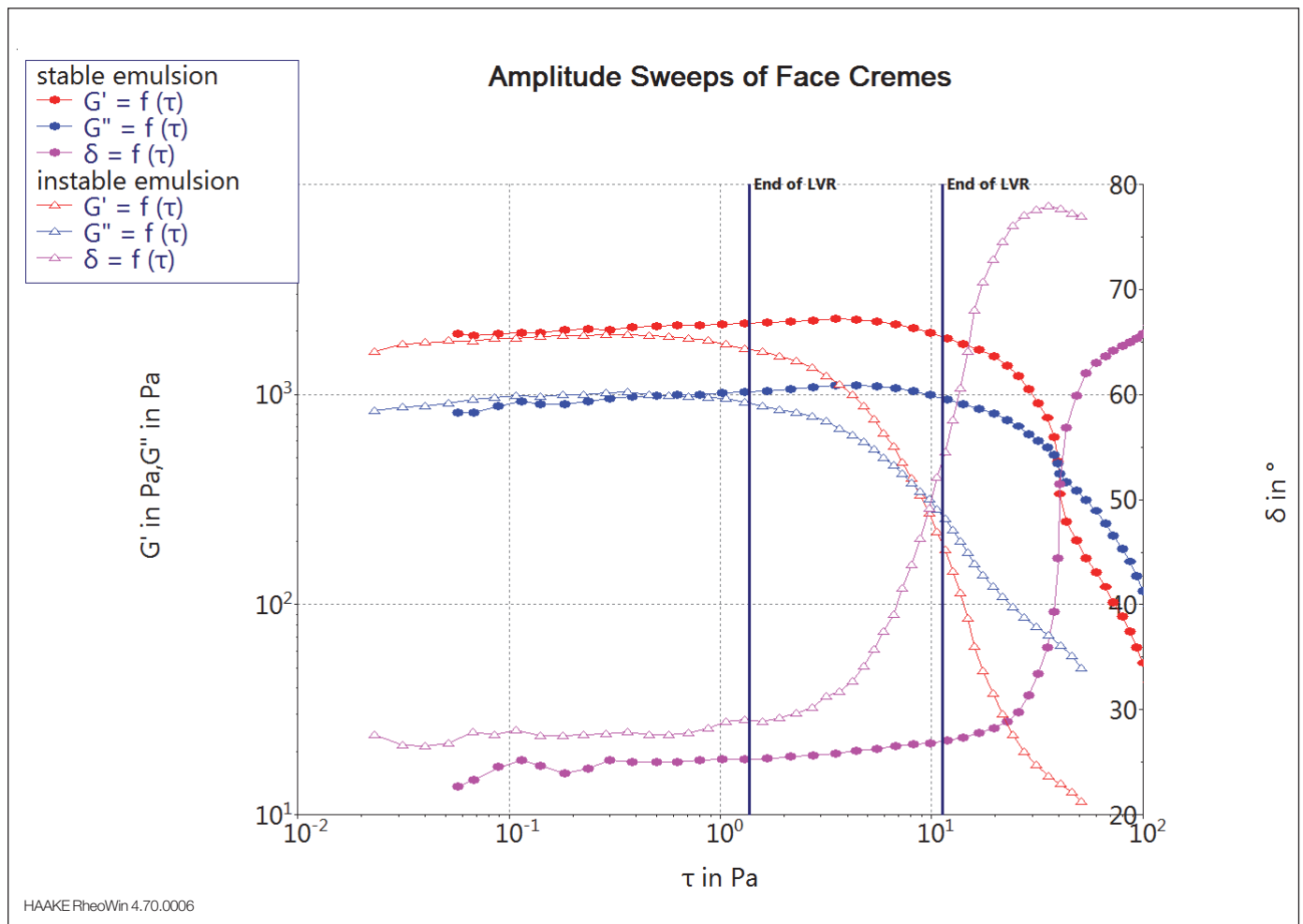


Fig. 2: Results of amplitude sweeps on 2 different cosmetic emulsions with the 2 perpendicular lines indicating the end of the respective linear viscoelastic range based on the storage modulus. For the less stable cream, the LVR ends at 1.4 Pa, for the stable cream it ends at 11.2 Pa.

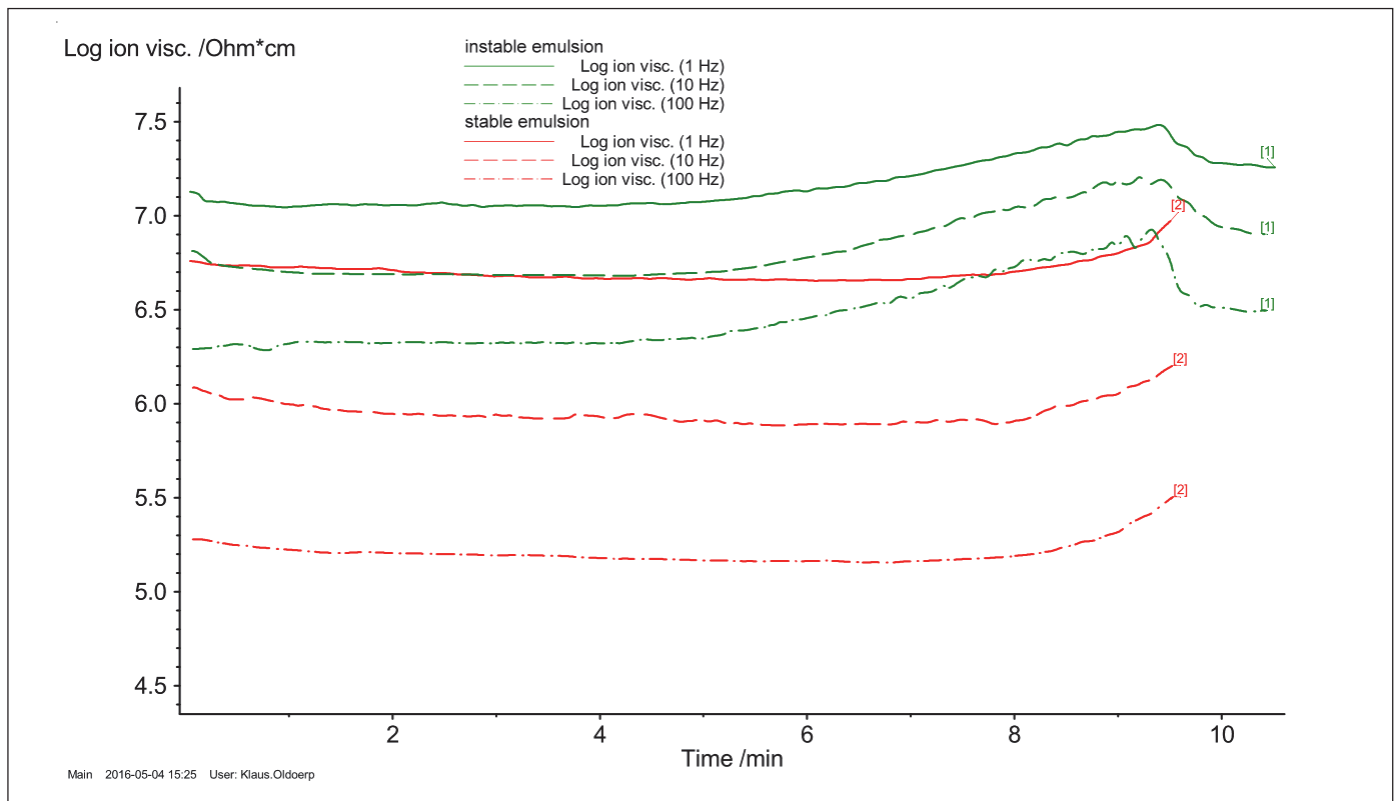


Fig. 3: Results of amplitude sweeps on 2 different cosmetic emulsions. The data is plotted over time since the Proteus software does not read the current rheometer status during the measurement.

Comparing the results from the temperature runs on the rheometer, the 2 creams behave in a similar way, with the less stable cream being less elastic throughout the whole measurement (Fig. 4). After having almost constant elasticity as indicated by the almost constant phase angle (δ), both samples start to lose elasticity above 12 °C. The only significant difference lies in the

maximum of δ above 30 °C. At 33 °C the phase angle of the less stable cream reaches a maximum and starts decreasing until the end of the measurement. For the stable cream, the maximum occurs at 35 °C and afterwards the decreasing part of the curve runs almost identical with the curve of the less stable cream.

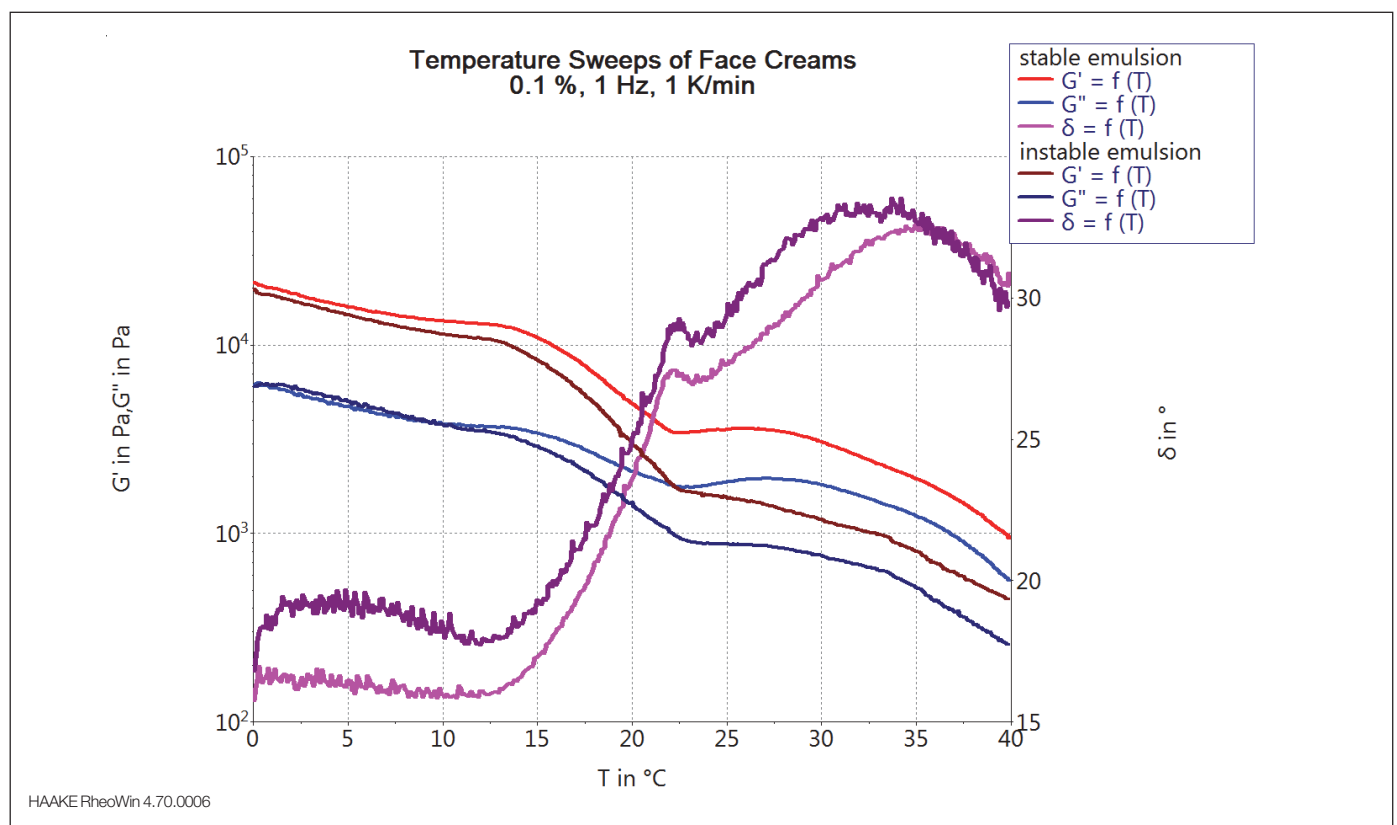


Fig. 4: The change in temperature dependent behaviour of both creams is almost the same with the less stable cream being less elastic.

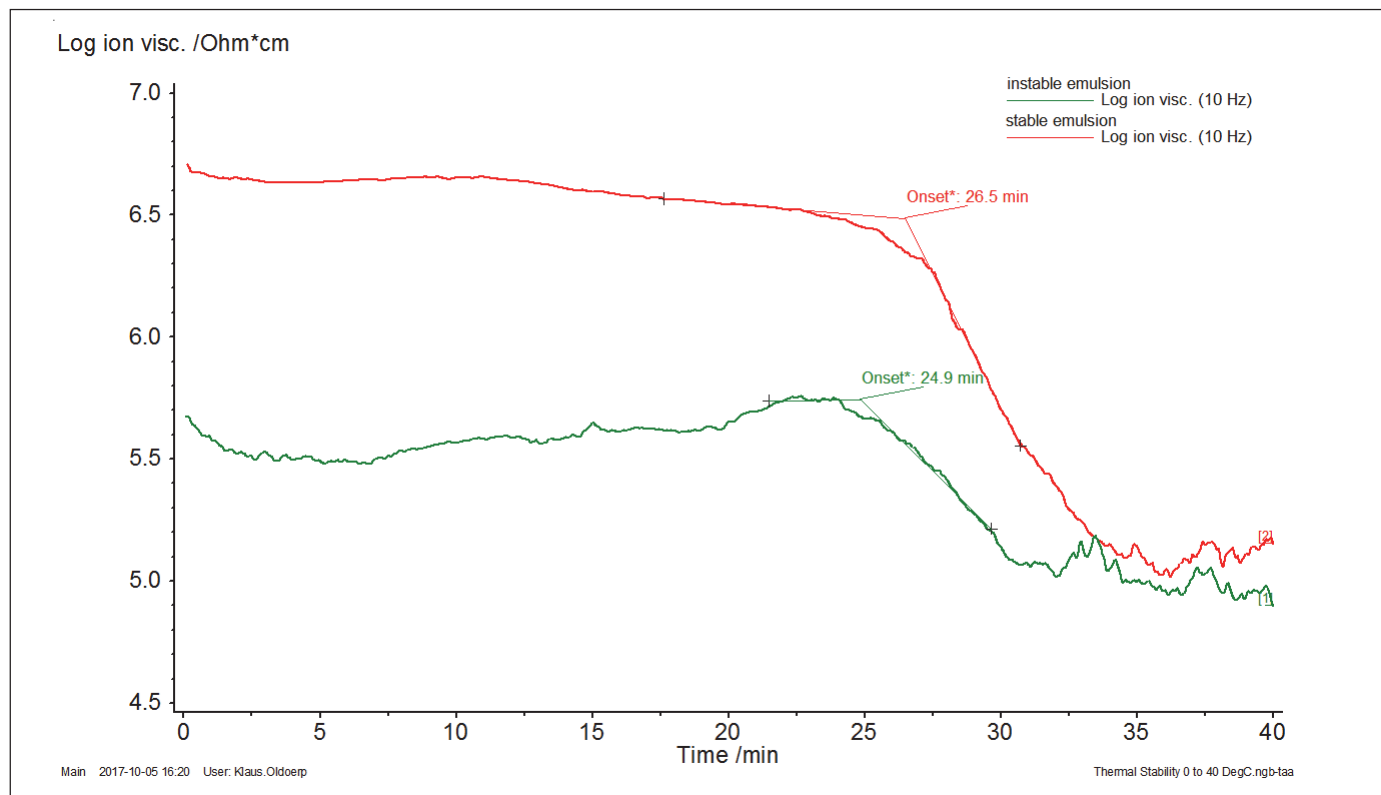


Fig. 5: Results of amplitude sweeps on 2 different cosmetic emulsions. Due to the temperature range from 0 °C to 40 °C, the time axis can accidentally be used as a temperature axis as well.

Comparing the DEA results collected during the temperature increase, the stable cream shows a higher ion viscosity before the values start to drop at 26 °C (Fig. 5). The corresponding curves of the less stable cream already go down from 24 °C on. These changes occur at a temperature, where the rheological curves do not show any similar change. Whether it is a coincidence to find the same temperature difference here like between the maxima of the phase angle in Fig. 4 cannot be answered based on the data available here.

The DEA results confirm the finding that the behaviour of both creams becomes the same above 34 °C. A possible interpretation of the combined information could be that the stable cream has a better homogeneity with smaller droplets of the aqueous phase, which would explain the higher initial ion viscosity. The less stable cream seems to have a more coherent water phase from the beginning on and therefore the lower initial viscosity. Above 34 °C the temperature-induced coalescence leads to the same conditions in both creams and hence the same properties.

Summary

With the HAAKE MARS, the two different creams have successfully been characterized. The visual difference between both products has been confirmed with significant differences in their mechanical response to different forces (stresses) and temperatures. The results from the DEA delivered additional information, which helps to explain why the differences exist and can be used as starting point for an analysis why these differences appeared based on the formulation, temperature history, homogenisation technique used or other process parameters.

Reference

- [1] Thermo Fisher Scientific product information P060
"Standard measuring geometries with integrated DEA-sensor for the HAAKE MARS rheometer platform"
Cornelia Küchenmeister-Lehrheuer, Klaus Oldörp

Find out more at thermofisher.com/rheometers

ThermoFisher
SCIENTIFIC

Investigating cocoa butter crystallization using simultaneous rheology and Raman spectroscopy (RheoRaman)

Author

Nathan C. Crawford and
Mohammed Ibrahim
Thermo Fisher Scientific
Madison WI, USA

Keywords

Cocoa butter, crystallization, Raman spectroscopy, rheology, RheoRaman, *in situ*, storage modulus G' , loss modulus G''

Thermo Fisher Scientific solutions

- HAAKE MARS 60 rheometer
- iXR Raman Spectrometer
- HAAKE RheoRaman module
- OMNIC for Dispersive Raman software

Application benefits

Simultaneous rheology and Raman spectroscopy measurements were used to examine the isothermal crystallization of cocoa butter (CB). The results indicate that CB crystallized by first hardening into an amorphous solid. The amorphous solid then underwent a morphological transition to form a crystalline solid. Without coupling these two separate analytical techniques, the observed amorphous-solid to crystalline-solid transformation would have been left undetected. Alone, each technique suggests a single-stage process, however, only when the two techniques are coupled is the multi-phase crystallization process revealed, further exemplifying the unique analytical capability unleashed by hyphenating rheology with *in situ* Raman spectroscopy.

Introduction

Cocoa butter (CB) is an edible vegetable fat extracted from the cocoa bean. CB is commonly used in home and personal care products (such as ointments and lotions) and CB is a vital ingredient in chocolate. CB forms the continuous phase within chocolate confections and is responsible for the chocolate's texture, snap, gloss, melting behavior, and resistance to fat bloom. These physical characteristics are a direct result of CB's triacylglycerol (TAG) composition and overall crystalline structure.

In general, TAG molecules assume a tuning fork configuration and the TAG "forks" assemble to form crystal lattice structures. During crystallization, the TAG molecules slow down as the CB oil cools and the TAGs come to rest in contact with one another, forming what are known as "sub crystalline cells."¹ Once the sub-cells are formed, they are thermodynamically driven to aggregate into larger and more stable crystalline structures.² The self-assembly of sub-cell structures and their further aggregation is governed by a balance of intra- and inter-molecular interactions. Depending on the molecular level packing and orientation of the TAGs, CB can form different types of crystal lattice structures (or polymorphs), where some crystal structures are more desirable than others. Overall, CB crystallization is a highly complex, multistage process. Understanding the isothermal crystallization behavior of CB is vital for improving chocolate manufacturing processes and maintaining product quality.

In this note, rheology coupled with *in situ* Raman spectroscopy was used to examine the isothermal crystallization of cocoa butter. Raman spectroscopy is a highly sensitive, relatively fast, and nondestructive technique that can probe the molecular structure and conformation in both liquid and solid TAG assemblies, as well as intra- and inter-TAG interactions. With simultaneous Raman spectra and rheological data, molecular-level interactions and conformational shifts during the isothermal crystallization of CB were directly correlated with the changes in bulk viscoelastic properties, providing unique insight into the multifaceted crystallization behavior of cocoa butter.

Materials and methods

Materials

Commercially available, organic cocoa butter (*Theobroma cacao*) was acquired from Inesscents™ (Ashland, OR, USA).

Rheology

Rheological measurements were performed using a Thermo Scientific™ HAAKE™ MARS™ 60 Rheometer equipped with a serrated 35 mm diameter plate rotor at a gap height of 1 mm. The serrated plate was used to prevent slip at the sample-rotor interface. All measurements were conducted in the oscillatory mode, with a frequency of 1 Hz and a constant strain of 0.1%. CB samples were loaded onto the rheometer at 60 °C and allowed to equilibrate for 10 min to erase any crystal structures and/or shear history from sample loading. After the equilibrium step, the temperature was rapidly decreased from 60 °C to 22 °C at a rate of 10 °C/min. The temperature was then held constant at 22 °C for 120 min, collecting data every 10 s.

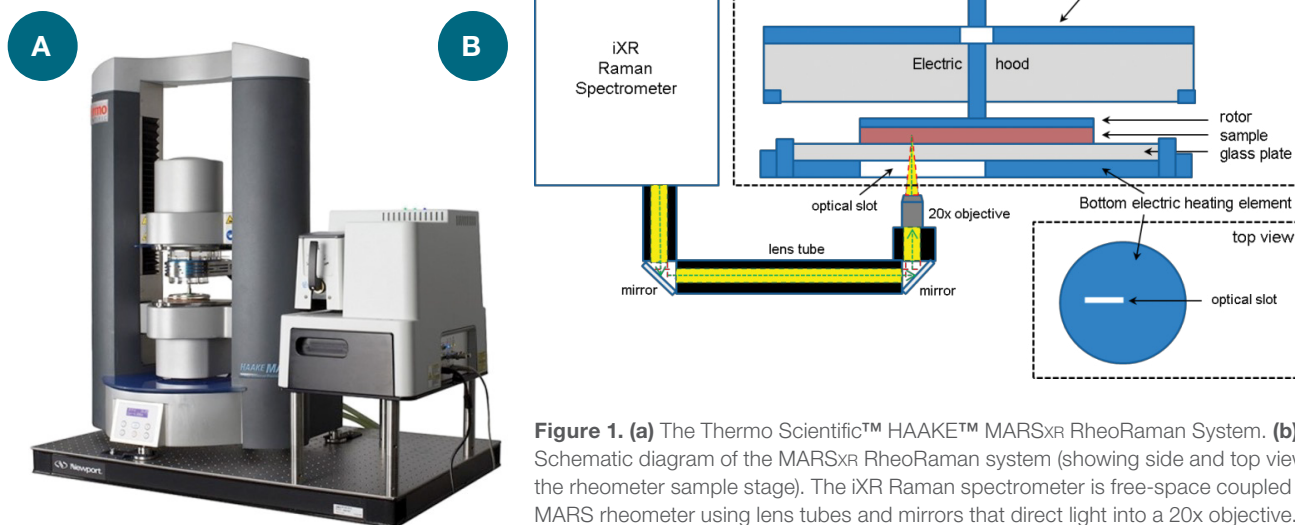


Figure 1. (a) The Thermo Scientific™ HAAKE™ MARSxR RheoRaman System. **(b)** Schematic diagram of the MARSxR RheoRaman system (showing side and top views of the rheometer sample stage). The iXR Raman spectrometer is free-space coupled to the MARS rheometer using lens tubes and mirrors that direct light into a 20x objective. The objective focuses the incoming laser (green dashed line) and collects the back-scattered Raman light (yellow) coming out of the sample sitting atop the rheometer stage.

Raman spectroscopy

Raman spectroscopy measurements were performed using a Thermo Scientific™ iXR™ Raman Spectrometer. A 532 nm laser was used with 10 mW laser power at the sample. The spectral range was 50-3500 cm^{-1} . The spectra were collected using a 2-second exposure time and 4 sample exposures. Data acquisition and processing were controlled by the Thermo Scientific™ OMNIC™ Software for Dispersive Raman. For the data presented here, Sequential Raman spectra (in parallel with the Rheological measurements) were collected over a predetermined time window using the time series collection function of the SERIES software within the OMNIC for Dispersive Raman software package.

RheoRaman coupling

The Thermo Scientific™ HAAKE™ MARSxR RheoRaman System consists of the iXR Raman spectrometer and the HAAKE MARS 60 rheometer coupled together using the HAAKE RheoRaman module (Figure 1a). The iXR Raman spectrometer was free-space coupled to the rheometer with an optical train which used a series of mirrors to direct the incident laser into the RheoRaman module (Figure 1b). Within the module, a mirror directed the laser beam into a 20x objective, where the laser light was focused into the sample (perpendicularly to the flow or vorticity plane). Backscattered Raman light was collected using the same 20x objective and guided back to the spectrometer using the same optical train as the incident laser (eventually to the spectrograph inside the spectrometer; Figure 1b).

The sample was positioned between a sandblasted glass bottom plate and the serrated 35 mm plate rotor (the textured plates were used to avoid slip at the sample-plate interfaces). An electrical heating element within the RheoRaman module provided temperature control from below the sample, while an active electrical hood was used to provide temperature control from above (eliminating the potential for a temperature gradient within the sample). Cooling of the sample was supplied from a temperature-controlled water bath circulator.

Results and discussion

Raman spectroscopy: Cocoa butter crystallization

Raman spectra for the liquid phase CB melt and the crystalline solid CB in the 500–3100 cm^{-1} range are shown in Figure 2. Prominent Raman features were observed in both the C–H stretching region (2700–3050 cm^{-1}) and the fingerprint region (1000–1800 cm^{-1}). More specifically, the lower Raman shift features include: the carbonyl (C=O)

stretching region (1700–1800 cm^{-1}), the olefinic (C=C) band at ~ 1655 cm^{-1} , the CH_3 and CH_2 deformations (~ 1460 and 1440 cm^{-1} , respectively), the CH_2 twisting region (1250–1300 cm^{-1}), and the C–C stretching region (1000–1200 cm^{-1}).

The C–H stretching regions for the melted and solidified CB specimens are highlighted in Figure 3. Two strong peaks were observed at ~ 2850 cm^{-1} and 2882 cm^{-1} , which are attributed to symmetric and asymmetric CH_2 stretching, respectively.² The symmetric vibrational modes at 2850 cm^{-1} were dominant in the liquid (melt) phase, while the asymmetric vibrations at 2882 cm^{-1} were dominant in the solid phase. Thus, the 2850 cm^{-1} and 2882 cm^{-1} bands are strong indicators of amorphous and crystalline content, respectively.³ Subsequently, the I_{2882}/I_{2850} peak intensity ratio was used to dynamically track crystal formation during the *in situ* RheoRaman measurements.

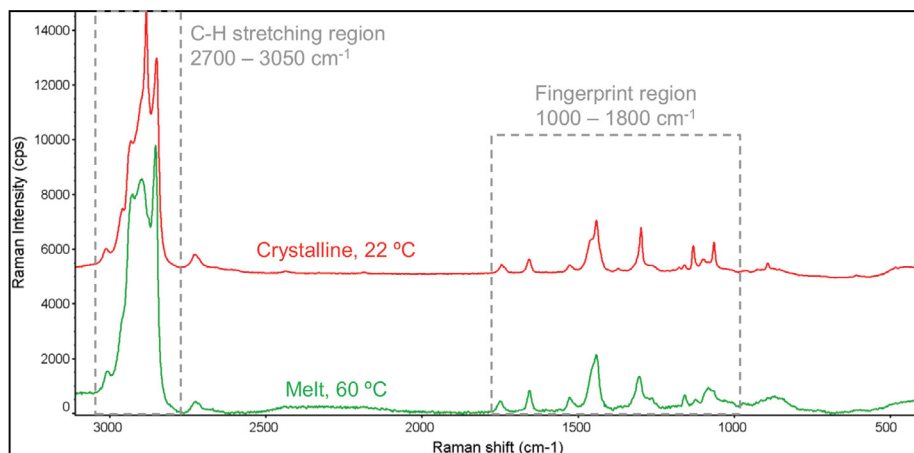
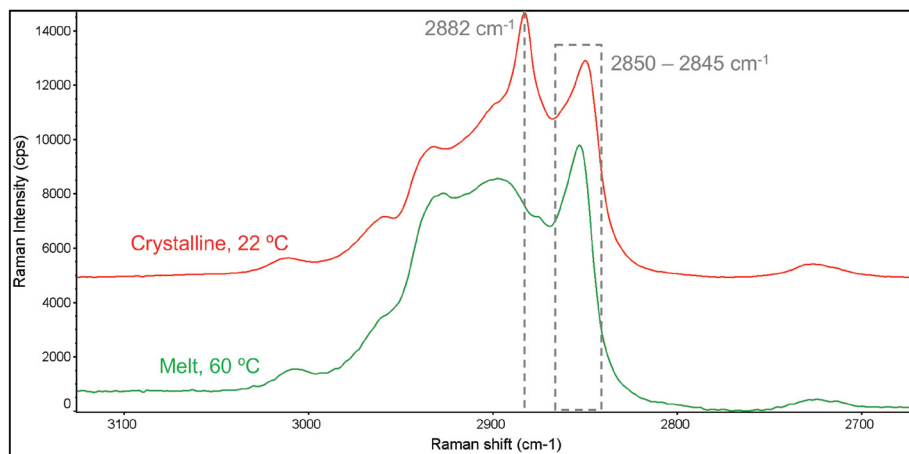


Figure 2. The full Raman spectra of melted and crystalline cocoa butter.

Figure 3. Raman spectra of the C–H stretching region (2700–3050 cm^{-1}) for melted and crystalline cocoa butter.



Although less intense than the C–H stretching region, approximately eight unique spectral features were identified in the fingerprint region (1000–1800 cm^{-1} ; Figure 4). When comparing the CB melt state to the crystalline phase, the most significant changes were observed in the C–C stretching region (1000–1200 cm^{-1}).

Two well-defined features emerged at 1130 cm^{-1} and 1063 cm^{-1} during the solidification process, which originate from the symmetric and asymmetric C–C stretching, respectively.^{4,5} In the melt phase, all C–C stretching bands were relatively weak and broad due to the disordering effects of methyl gauche conformations.

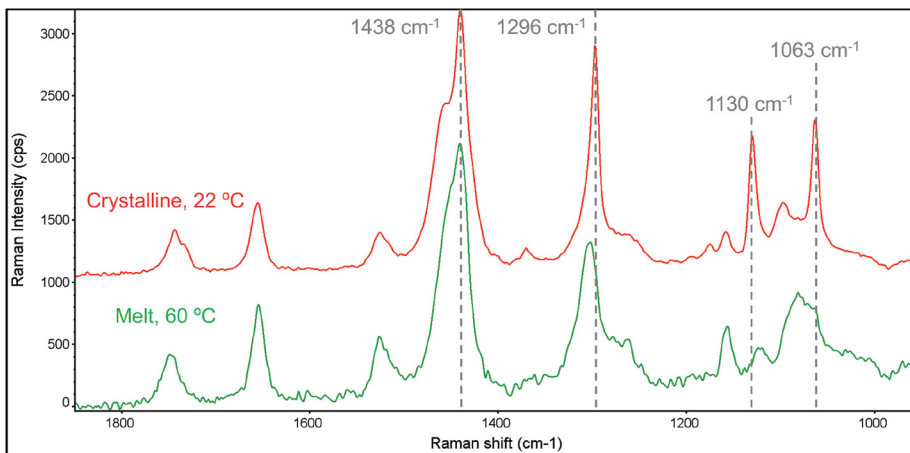


Figure 4. The 1000–1800 cm^{-1} Raman spectral range for melted and crystalline cocoa butter.

However, as the CB solidified, the backbone methyl groups were ordered into the trans-conformation, signified by the emergence of the peak at 1130 cm^{-1} . Therefore, in addition to the I_{2882}/I_{2850} peak intensity ratio, the I_{1130}/I_{2850} spectral marker was also used to track the crystalline-phase transition within CB via *in situ* rheoRaman measurements.

Simultaneous rheology and Raman spectroscopy (RheoRaman)

The melt-to-solid phase transition of cocoa butter was probed rheologically using small amplitude oscillatory shear measurements (Figure 5a), where the storage modulus G' and loss modulus G'' were measured as a function of time at the isothermal temperature of 22°C . G' and G'' are measures of a material's elastic and viscous behavior, respectively. A liquid-like material will be more viscous than elastic (i.e., viscously dominated), and as a result, G'' will be greater than G' . Conversely, a solid-like material will display more elastic than viscous behavior (i.e., elastically dominated), where G' will be greater than G'' . The overall magnitudes of G' and G'' , as well as their relative difference in magnitude, often reported as the ratio of G''/G' , determines the general viscoelasticity and overall resistance to deformation for a given material.

The ratio of G''/G' (plotted on the right y-axis of Figure 5a) is commonly used to track viscoelasticity of a material:

$$\frac{G''}{G'} = \tan(\delta),$$

where δ is the phase angle defined as the shift or lag between the input strain and resultant stress sine waves (or vice versa) during an oscillatory shear measurement. The term “ $\tan(\delta)$ ” is often referred to as the loss or damping factor. Values of $\tan(\delta)$ less than unity indicate elastically dominant (solid-like) behavior, while values greater than unity indicate viscously dominant (liquid-like) behavior.

Unlike the individual moduli, $\tan(\delta)$ can be used to quantify overall brittleness of a material and is commonly used to assess glass transition behavior. In general, as $\tan(\delta)$ becomes smaller, the more G' deviates from G'' , and the more brittle (or glass-like) the material becomes.

During the initial portion of the isothermal hold at 22°C from 0 to 5 min (immediately following the rapid decrease in temperature from 60°C to 22°C), both G' and G'' increased as the CB transformed from a melted liquid to a soft semi-solid (Figure 5a). This initial increase in modulus is most likely due to a delay between the set temperature and the internal temperature of the loaded sample. Once the sample had reached thermal equilibrium and was at the isothermal set point of 22°C , the moduli were relatively stable from 10 to 25 min. From 25 to 50 min, however, both G' and G'' begin to gradually increase and then from 50 to 80 min, the moduli rapidly increased, where G' and G'' increased by approximately 5 and 4 orders of magnitude, respectively. The exponential increase in the moduli indicates a solidification process, where the CB transformed from a pliable semi-solid to a more robust, hardened solid. At 80 min and beyond, growth in the elastic modulus slowed and eventually plateaued, showing no further significant change past 100 min. The viscous modulus, however, reached a slight plateau from 80 to 100 min and then proceeded to gradually decrease from 100 min and beyond.

During the increase in G' and G'' , a rapid decrease in the loss factor $\tan(\delta)$ was observed from ~65 min and beyond (Figure 5a, right y-axis). The decrease in the loss factor indicates a deviation in overall magnitude between G' and G'' . As the CB hardened, the increase in G' exceeded the increase in G'' , triggering the decrease in $\tan(\delta)$. At the end of the 120 min isothermal study, G' was more than a full order of magnitude greater than G'' and the loss factor was approaching 0.01, indicating the CB had transitioned into a brittle glass-like solid.

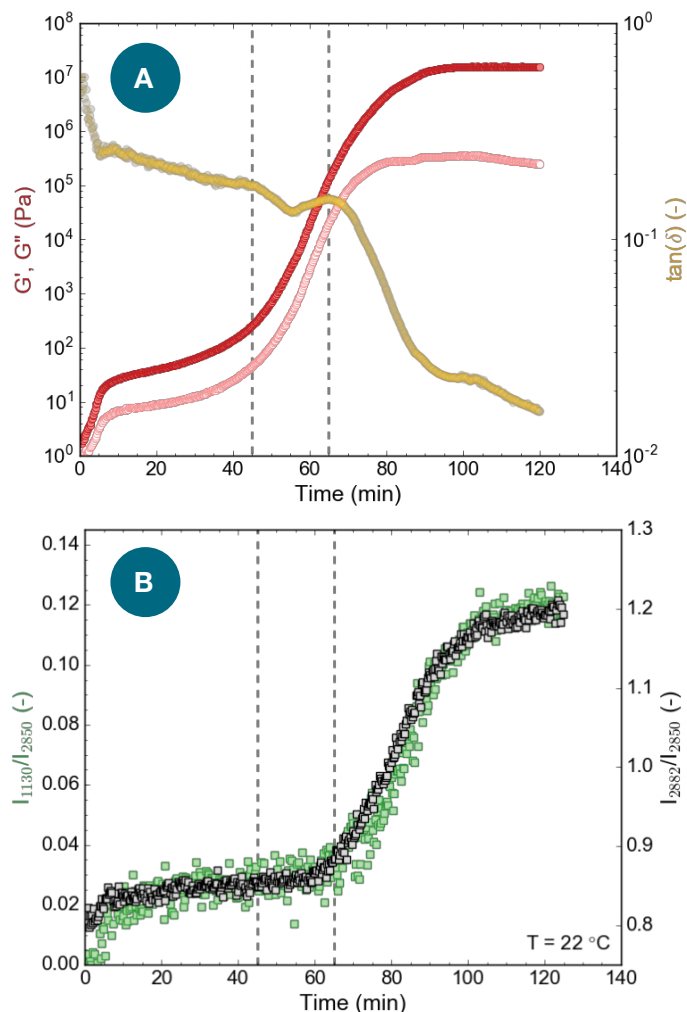


Figure 5. (a) Rheology: G' and G'' (filled and open circles, respectively; plotted on the left y-axis) and $\tan(\delta)$ (plotted on the right y-axis) and **(b)** Raman: the I_{1130}/I_{2850} (left y-axis, green) and I_{2882}/I_{2850} (right y-axis, black) peak intensity ratios for CB during isothermal crystallization at 22 °C. The vertical dashed line at 45 min indicates the increase of G' and G'' , while the dashed line at 65 min indicates the decrease in $\tan(\delta)$ and increase in the Raman ratios.

The observed rheological behavior was further confirmed using simultaneous Raman spectroscopy (Figure 5b). Initially, both the I_{1130}/I_{2850} and I_{2882}/I_{2850} peak intensity ratios remained unchanged during the first ~65 min of the isothermal study. Then a sharp increase of the I_{1130}/I_{2850} and I_{2882}/I_{2850} ratios began at ~65 min, indicating the formation of crystal structures within the CB. As the CB further crystallized, both spectral markers continued to increase from 65 to 100 min. Beyond 100 min, the growth in both Raman features had subsided and the peak intensity ratios began to stabilize.

Overall, the rate of increase in the 1130 and 2882 cm^{-1} spectral ratios were similar to the rate of change for both G' and G'' (i.e., they increased with similar slopes). However, there was a noticeable 15-20 min lag between the observed increase in G' and G'' and the rise of the Raman intensity ratios. The sharp upturn in G' and G'' indicates an increased resistance to deformation (i.e., a bulk hardening of the CB), signaling the start of the solidification process. The

Raman spectral markers, on the other hand, are indicators of crystal formation. Thus, the time delay between the rheology and Raman profiles suggests that CB first hardens into an amorphous solid, followed by a transformation from an amorphous to a crystalline solid. This morphological transformation was signified by the subsequent increase in the Raman band intensities associated with crystal CB structures (the 1130 and 2882 cm^{-1} peaks). The temporal separation of the rheological and Raman spectral profiles indicates a clear distinction between bulk hardening of the CB and the formation of crystalline domains.

Interestingly, the increase in the Raman spectral features (I_{1130}/I_{2850} and I_{2882}/I_{2850}) directly correlated with the observed reduction in $\tan(\delta)$ (Figure 5a and b). The loss factor is an indication of material brittleness and crystalline structures are commonly known to be brittle. Thus, it is reasonable that the formation of crystal domains at the molecular level (as indicated by Raman) coincides with the overall brittleness of the CB. As a result, the loss factor may be a more revealing indicator of bulk CB crystallization than G' and G'' alone.

Conclusions

Simultaneous rheology and Raman spectroscopy measurements were used to examine the isothermal crystallization of cocoa butter. This multimodal analytical technique allowed the bulk mechanical properties of cocoa butter (G' , G'' , and $\tan(\delta)$) to be directly correlated with conformational changes at the molecular level ($\nu_{\text{as}}(\text{CH}_2)$ mode at 2882 cm^{-1} and the $\nu_{\text{s}}(\text{C-C})$ mode at 1130 cm^{-1}) in real-time. After rapid cooling (10 °C /min) and at an isothermal temperature of 22 °C, there was a noticeable time lag between the rheological response (G' and G'') and the Raman spectral profiles. The observed time delay indicates that CB crystallized by first hardening into an amorphous solid, manifested by a sharp increase in G' and G'' while the Raman features remained unchanged. The amorphous solid then underwent a morphological transition to form a crystalline solid, signified by the increase in Raman features associated with crystal CB structures (1130 and 2882 cm^{-1}). Without coupling these two separate analytical techniques, the observed amorphous-solid to crystalline-solid transformation would have been left undetected. Alone, each technique suggests a single-stage process, however, only when the two techniques are coupled is the multi-phase crystallization process revealed, further exemplifying the unique analytical capability unleashed by hyphenating rheology with *in situ* Raman spectroscopy. While this work focusses on the isothermal crystallization of CB, the underlying principles applied here should be applicable for a wide range of material processes including gelation, polymerization, curing behavior, as well as other shear-induced phenomena.

References

1. K. Sato, *Crystallization of Lipids: Fundamentals and Applications in Food, Cosmetics, and Pharmaceuticals*. Hoboken, NJ: John Wiley & Sons, 2018.
2. S. Bresson, D. Rousseau, S. Ghosh, M. El Marssi, and V. Faivre, *Raman spectroscopy of the polymorphic forms and liquid state of cocoa butter*, Eur. J. Lipid Sci. Technol. 113, 992–1004, 2011.
3. R. G. Snyder, H. L. Strauss, and C. A. Elliger, *C–H stretching modes and the structure of n-alkyl chains*. 1. Long, disordered chains, J. Phys. Chem. 86, 5145–5150, 1982.
4. R. J. Meier, *Studying the length of trans conformational sequences in polyethylene using Raman spectroscopy: A computational study*, Polymer. 43, 517–522, 2002.
5. M. Zheng and M. Du, *Phase behavior, conformations, thermodynamic properties, and molecular motion of multicomponent paraffin waxes: A Raman spectroscopy study*. Vib. Spectrosc. 40, 219–224, 2006.

Find out more at

www.thermofisher.com/Raman

www.thermofisher.com/MARS

ThermoFisher
SCIENTIFIC

APPLICATION NOTE

The rheological behaviour of shampoos - What makes a product acceptable for a specific target customer?

Authors

Jan Philip Plog
Thermo Fisher Scientific, Karlsruhe, Germany

Introduction

Shampoos are based on complex systems of surfactants having the function to cleanse the hair. Because of their everyday use it is not surprising that the shampoo market comprises approx. 12% of the total personal-care industry [1]. These products are complex systems consisting of about 80 wt.% water, 10wt.% surfactants, 5wt.% viscosity modifiers, 2wt.% preservatives, fragrances and colorants and about 3wt.% of performance additives [2].

Few things are more important to customers than using a thick (rich) shampoo product correlating this directly with value and concentration. A shampoo is not only expected to be easy to use but to meet also sensory criteria that will appeal to the customer. One main rheological parameter that correlates with the thickness and flow properties of a shampoo is the viscosity. The viscosity affects both the cleansing efficiency and the user perception of a shampoo product. In addition to that it also influences the foaming properties, production filling, packaging, storage and long-term stability of the product. Viscosity is a quite important parameter! As was mentioned already, customer perception is one of the most important parameters, however who is the customer and what does he expect? The three different customer groups Female, Male and Children (Infants) have different views on the same product class because they usually put different amounts of energy into a shampoo when they i.e., squeeze it out of the bottle or distribute it on themselves. This is due to the fact that the different processes will happen at different stress levels (as the customer groups apply different forces) and thus result in different shear rates. As no customer wants to experience the viscosity the product has at rest (rich and creamy) when they actually use the product, a shampoo has to be a non-Newtonian or to be more precise shear-thinning fluid. To induce non-Newtonian flow and thus modify the flow behaviour towards the specific customer groups, water-soluble polymers are used as modifiers.



This contribution is to show how products for those different customer groups differ rheologically and how easy it is to absolutely determine the parameter viscosity with the help of the Thermo Scientific™ HAAKE™ Viscotester™ iQ rheometer.

Methods and materials

Three different commercial shampoos have been tested on the Thermo Scientific HAAKE Viscotester iQ at room temperature with 35 mm plate/plate geometries (see Figure 1). One of them was a shampoo for men, one for women and one for children (infants).

After carefully filling the shampoo on the lower plate and manually adjusting the measuring head to a predetermined gap of 1 mm the testing procedure was conducted as can be seen in Figure 2.

With the described procedure the shampoo products have been tested in a shear rate range of 1 to 100 1/s, the results can be seen in Figure 3.

Results and discussion

As can be seen in Figure 3 the rheological fingerprint for the three products is quite different. At low shear rates around 1 1/s the shampoo for men and the shampoo for children (infants) have about the same viscosity of about 12 Pas. The shampoo for women has a considerably lower viscosity of about 7.5 Pas. Male customers usually want to have an even richer (higher viscous) product than female customers that prefer slightly “creamier” (lower viscous) products. For child products more functional aspects have to be taken into account as a child usually does not choose a shampoo according to its viscosity. However, the parents that buy the product intuitively “know” that a high viscous product will stay longer in the child’s hand when using it in the bathtub.

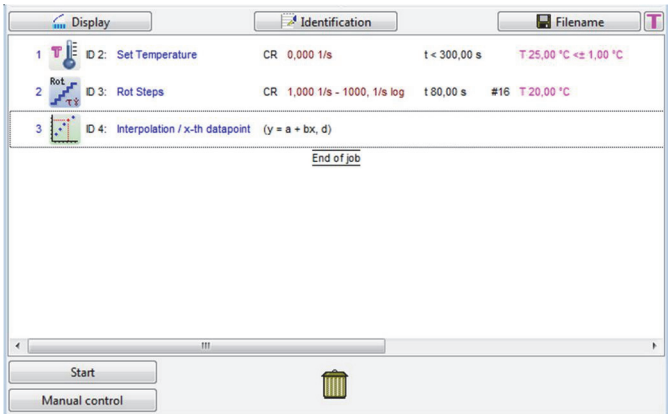


Fig. 2: HAAKE RheoWin Measuring Routine to determine the viscosity as a function of shear rate on the Thermo Scientific HAAKE Viscotester iQ.

When applying higher shear rates the behaviour differs between the products. Whereas the “male” product goes into non-Newtonian flow directly because of the higher molecular weight polymer additives that have been used in formulation to achieve a higher base viscosity, the “female” and “child” product show Newtonian plateaus. However whereas the “female” product leaves Newtonian flow at around 4 1/s to achieve lower viscosities when being used the “child” product maintains a constant viscosity for much longer (up until about 20 1/s) so that less product is lost before starting in the washing process.

Right now many users of viscometers, especially in an industrial QC/QA environment, are working with concentric cylinder measuring geometries (“cup and bob”). However, the use of plate/plate measuring systems is preferable because less sample volume is needed. This directly leads to two main advantages, namely that cleaning will be easier and temperature control will be faster. However do both measuring geometries yield the same result? To answer that question, Figure 4 shows the resulting viscosity for the “soft” shampoo measured at room temperature with the concentric cylinder system CC25Din in comparison to a 35 mm plate/plate geometry.

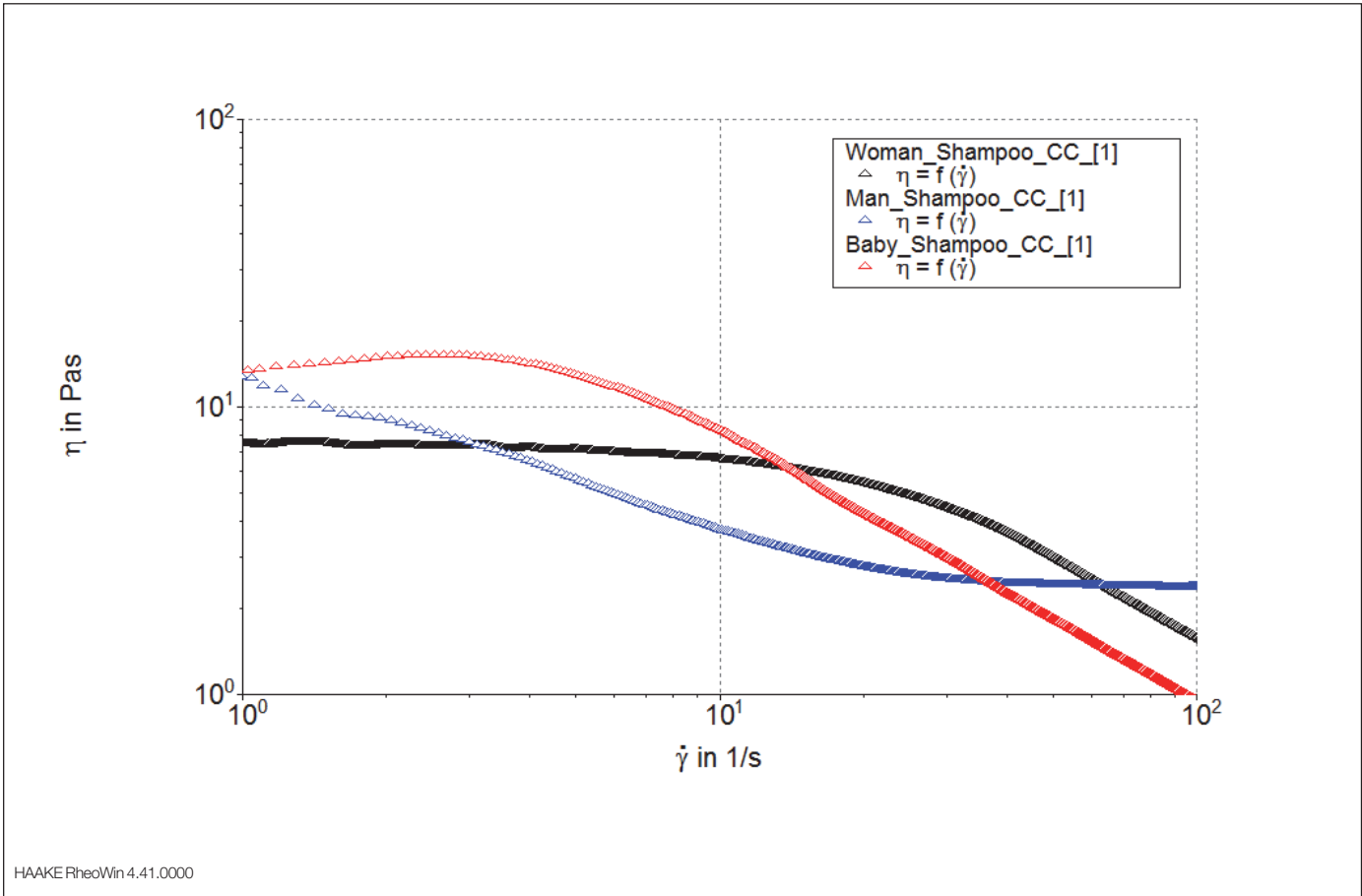
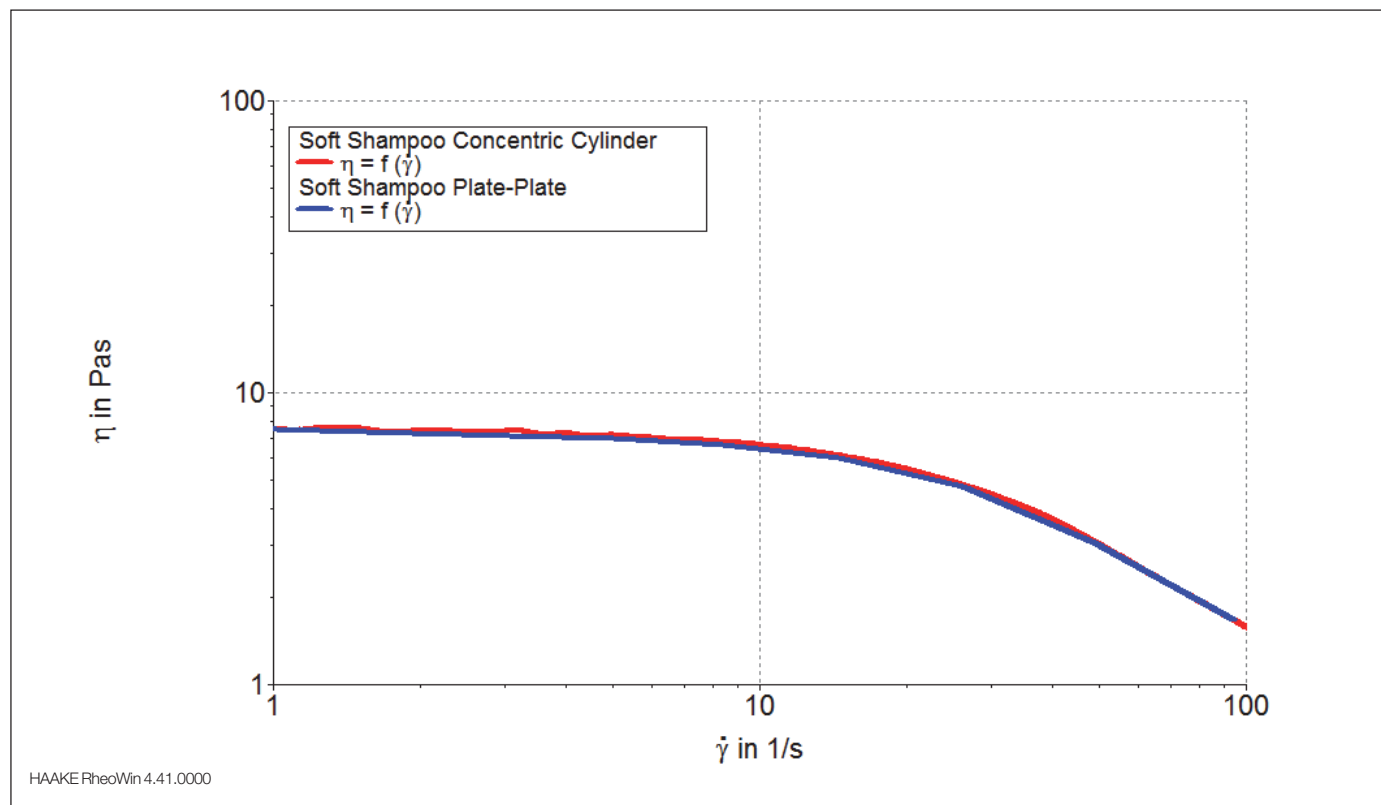


Fig. 3: Viscosity as a function of shear rate for three different shampoos at RT.

As can be seen in Figure 4, the measured viscosity is the same, independent of the measuring geometry.



Conclusion

Determining the viscosity of a shampoo (or shower gel etc.) formulation is of utmost importance to understand if a product meets customer expectation. Additives have to be chosen wisely to formulate a product for a specific customer group. The Thermo Scientific HAAKE Viscotester iQ rheometer is a powerful tool to let you conduct those tests easy and reproducible, no matter if you test with concentric cylinders or plate/plate geometries.

Literature

- [1] Drug Chain Review, 22, 2, 2000, 15-18
- [2] H. Leidreiter, U. Maczkiewitz, Utilizing Synergistic Effects in Surfactant Mixtures, Th Goldschidt AG, 1996, Essen

Find out more at thermofisher.com/rheometers

ThermoFisher
SCIENTIFIC

Product stability or shelf-life - What rheology has to do with it

Authors

Klaus Oldörp
Thermo Fisher Scientific, Karlsruhe, Germany

Introduction

Whenever two-phase systems like emulsions, suspensions or foams are used one of the most important questions is their long-term stability crucially important for example for a product's shelf-life. Depending on how much the 2 phases differ in density and chemical nature, it takes special preparation steps and/or additives to ensure a stable product.

Phase separation happens when one phase migrates through the other phase e.g. due to gravity or buoyancy. The flow behaviour of both phases is essential for the understanding of this process. A modification of at least one phase's flow behaviour can be used to reduce or suppress the phase separation.

To avoid e.g. sedimentation, the viscosity at low shear rates has to be high to slow down the sedimentation process. To stop the phase separation completely a yield stress can be introduced into the product either by selecting suitable components or by using suitable additives. Subsequently, rheology is one of the most important methods when formulating a new product or testing an existing one with a focus on its long-term stability.

Methods and materials

Measuring viscosities at low shear rates can be time consuming due to the longer equilibration times at low shear rates. To minimize the time necessary to record a viscosity curve it is important to use a rheometer, which is able to quickly reach the desired rotational speed and keep it constant even at the lowest speeds.

Results and discussion

Using its fast and precise speed control (Fig. 1) combined with its excellent torque sensitivity, the Thermo Scientific™ HAAKE™ MARS™ can record viscosity curves over a wide range of shear rates. Fig. 2 shows an example for a viscosity curve starting from a shear rate of 10^{-8} s^{-1} . Despite the fact that the shear rate spans a range of 10 orders of magnitude, the curve has been recorded using a single measuring geometry within a single run.

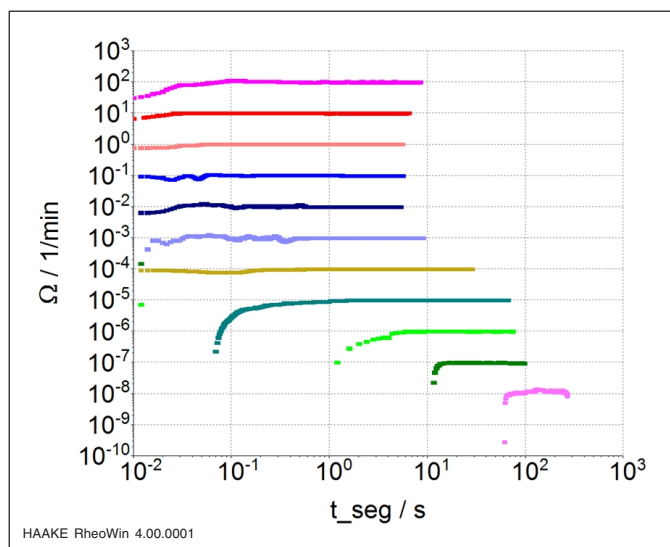


Fig. 1: Its modern control loop design allows the HAAKE MARS to quickly reach a constant rotational speed even at ultra low rates of 10^{-8} rpm.

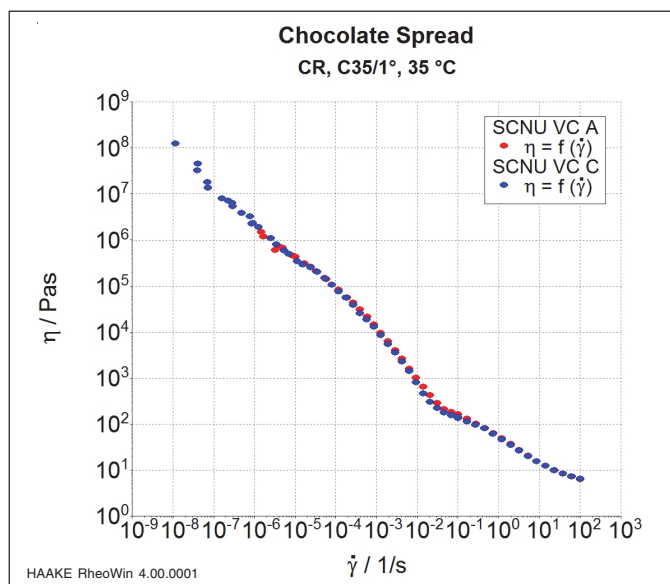


Fig. 2: Viscosity curve of a chocolate spread at 35°C over 10 orders of magnitude in shear rate. The viscosity drops by more than 7 orders of magnitude during the test.

The yield stress τ_0 is the stress level at which a material ceases to behave elastic and starts to flow. While a high viscosity at low shear rates is only able to slow down phase separation, a sufficiently high yield stress can fully prevent any sedimentation. The recommended test method for the yield stress is the stress ramp [1]. Its advantages are the continuous increase of stress on the sample, data is collected below and above the yield stress i.e. no extrapolation is needed and it is a sensitive method also suitable for smaller yield stresses.

To determine the yield stress a linear stress ramp is used. The ramping time is selected according to the sample's nature and should be chosen to reach the yield stress 2 – 3 min after its start.

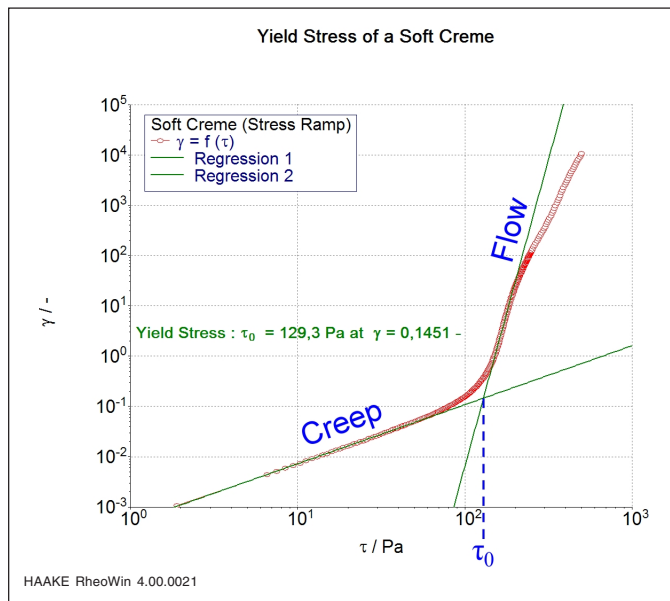


Fig. 3: Deformation as a function of stress during a linear stress ramp for a soft crème. The intersect of the curve's slope in the creep regime and the curve's slope in the flow regime marks the yield stress τ_0 .

With increasing yield stress a substance is able to bear stronger forces like e.g. the weight force of suspended particles without yielding. Since with increasing yield stress a substance also becomes less flexible it is important to find the optimum value to have a good stability without losing the smoothness needed for the respective application like for a cosmetic emulsion, a lubricant or a specific food product. Fig. 3 shows a typical example of a yield stress test result of a cosmetic emulsion. The measuring and evaluation software Thermo Scientific™ HAAKE™ RheoWin™ fits 2 tangents to the curve's respective creep and flow regime and takes their intersect as the yield stress.

The value obtained can be correlated with the forces trying to destabilize the material like e.g. the sedimentation stress τ_s that a particle puts on the fluid (Fig. 4) to calculate whether sedimentation will occur or not.

Since some experience is needed for selecting the best parameters and the data evaluation, some users shy away from this test method and look for alternatives. A method,

which got some attention due to its simplicity, is to run an oscillation amplitude sweep on the sample and use the end of the linear viscoelastic range (LVR) as a number related to the yield stress (see Fig. 5).

$$\tau_s = \frac{r \cdot g (d - \rho)}{3}$$

$\tau_s > \tau_0 \Rightarrow$ sedimentation
 $\tau_s < \tau_0 \Rightarrow$ no sedimentation

Fig. 4: The sedimentation stress τ_s a particle puts on the liquid below it depends on its size and the difference between the particle's density and the liquid's density.

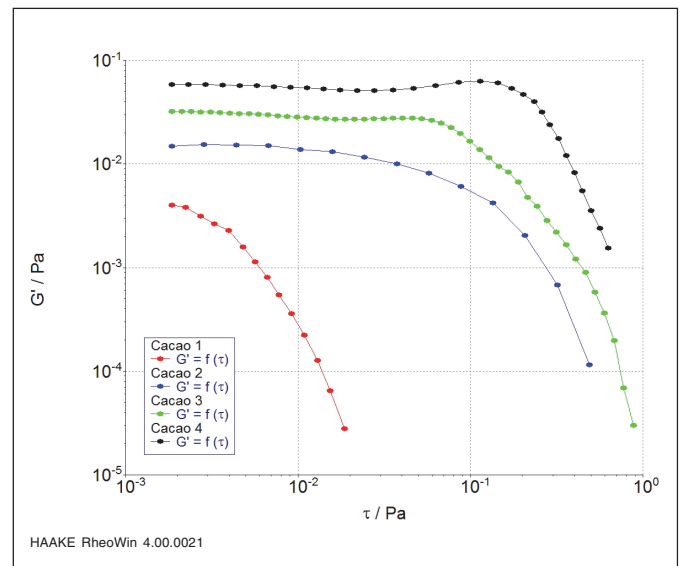


Fig. 5: Linear viscoelastic range of different cacao milks. Sample 4 (black curve) is the most stable against sedimentation.

To use this method is tempting because the end of the LVR is usually easily accessible and the results show good reproducibility. Still, it has to be kept in mind that the length of the LVR depends on the oscillatory frequency used and is therefore a relative number only. Even worse, this test does not apply a steadily increasing stress to the sample, which would be the logical consequence of the definition of the yield stress. With an oscillation test, a continuously changing stress is applied for every data point, a completely different way of stressing the sample.

Subsequently the value determined from the oscillation test differs from the yield stress determined with the stress ramp. It is therefore vitally important to agree on a common method before comparing yield stress values.

Conclusion

Rheology is an essential tool when testing the long-term stability of a liquid or paste-like product. The viscosity at low shear rates and the yield stress can be used to reduce or to prevent sedimentation. Due to its torque sensitivity and precise speed control, the HAAKE MARS is an excellent choice to determine these parameters with high precision in a very time efficient way.

Reference

- [1] DIN Technical Report No. 143 of the NPF/NAB-AK 21.1
"Rheology", Modern Rheological Test Methods - Part 1:
Determination of the Yield Point - Fundamentals and
Comparative Testing

Find out more at thermofisher.com/rheometers

The logo for ThermoFisher Scientific, with "ThermoFisher" in red and "SCIENTIFIC" in black.

Investigating the viscoelastic behavior of cosmetic emulsions by performing creep and recovery tests

Author

Fabian Meyer
Thermo Fisher Scientific, Karlsruhe, Germany

Introduction

Understanding the complex flow and deformation behavior of cosmetic emulsions helps to design and optimize final products, to meet the consumer expectations in terms of appearance and behavior during application. Rotational rheometers are the ideal instruments to investigate the rheological properties of liquid and semi-solid formulations. Rheological tests can also be used to simulate processing condition to make production more efficient as well as to assess product stability and shelf life behavior.

For complex materials, like for instance all types of dispersed systems, we differentiate in general between their viscous and elastic properties. Both contribute to the overall flow and deformation behavior and the perception of a material during application. A various number of test methods are available to measure the response of a material to an external mechanical excitation.

Theoretical background

Creep and recovery tests are the most direct way in rheology to qualify and quantify the elasticity of a material. The experiment is divided into two segments. During the first part, the creep, an instantaneous stress signal is applied to the sample for a defined period of time. In the second part, the stress is removed again and the recovery of the sample is monitored. The response of the sample is a deformation curve with a shape depending on both, the amount of stress applied by the rheometer and the microstructure of the sample. For pure viscous and pure elastic materials the results of a creep and recovery experiment are shown in Figures 1a and b, respectively.

For a pure viscous material the deformation increases linearly over time as long as a constant stress signal is applied. The constant slope of the deformation signal indicates steady shear conditions over the entire creep phase.

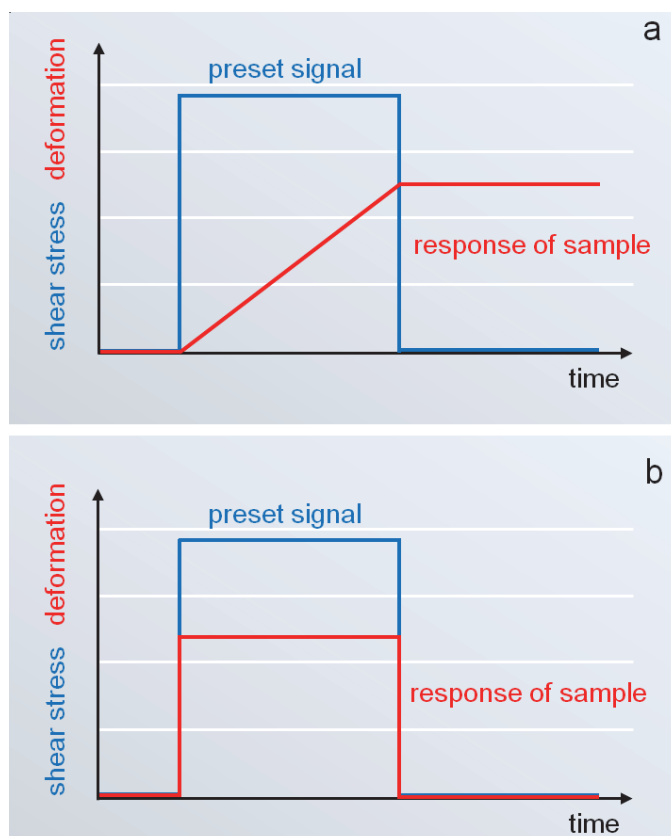


Fig. 1: Behavior of a pure viscous (a) and a pure elastic (b) material in a creep and recovery test.

Once the stress is removed from the viscous sample the deformation signal will remain constant and no back-deformation is observed (Fig. 1a). All kinetic energy brought into the material during the creep phase dissipates into heat energy and is not stored in the material. The viscous material does not show any elastic response. The other extreme behavior is the one of a completely elastic material. When neglecting all effects caused by the instrument and sample inertia, this type of material shows an instantaneous and constant deformation once a constant stress is applied.

In the recovery phase the deformation jumps back to zero (Fig. 1b). The back-deformation is a result of the elasticity of the material. All energy is stored inside the material and released again once the stress is removed.

Most complex materials do not behave like an either purely viscous fluid or a purely elastic solid. They exhibit both, viscous and elastic behavior. The degree of the two components depends on the characteristics of the sample as well as the magnitude of applied stress. The results of a creep and recovery test with an ideal viscoelastic sample are shown in Figure 2.

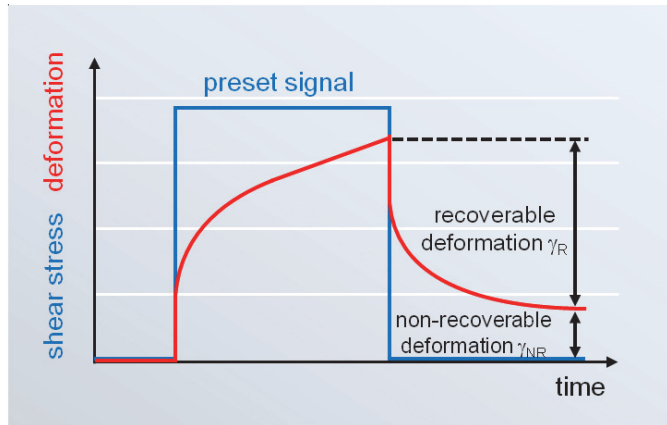


Fig. 2: Behavior of an ideal viscoelastic material in a creep and recovery test.

The deformation curve can be divided into different sections. During the creep part the viscoelastic material shows an instantaneous increase in deformation as a first response. This can be assigned to initial elastic stretching of the structural units of the sample. The second part is a viscoelastic response, where first changes to the microstructure are occurring. Once all elastic components are fully stretched, a steady state flow with a linear increase of the deformation signal over time is observed. When the stress is removed an instantaneous elastic back deformation, followed by a delayed viscoelastic deformation is observed. After a certain period of time a constant value is reached and the sample is fully recovered again. As shown in Figure 3, the total deformation of the material during the creep phase can be separated into two categories: the recoverable deformation γ_R and the non-recoverable deformation γ_{NR} . The more elastic a material behaves, the more recoverable deformation can be observed during the recovery part. It is important to note that percentage of recoverable deformation (in comparison to the total deformation) for a viscoelastic sample will decrease the longer the duration of the steady state flow during the creep period. A more absolute measure of the total elasticity of a material is the so called equilibrium compliance J_e . The equilibrium compliance is the ratio of the recoverable deformation and the applied stress during the creep phase:

$$J_e = \gamma_R / \tau$$

[1]



Fig. 3: HAAKE Viscotester iQ Air with Peltier temperature control.

Materials and methods

In order to measure the recoverable deformation of a material correctly, a rheometer with a low friction bearing should be used. Instruments with a mechanical bearing will in general show a too low recoverable deformation since some of the energy stored inside the sample is needed to overcome the internal friction of the rheometer. This is especially true for materials that exhibit a very fragile structure and only low elasticity.

The results presented in this report were obtained using the Thermo Scientific™ HAAKE™ Viscotester™ iQ Air rheometer in combination with a Peltier temperature control unit for parallel plates and cone & plate geometries (Figure 3). Several creep and recovery tests were performed on a commercially available soft cosmetic emulsion. A 60 mm 1° degree cone measuring geometry was used for all measurements. All tests were performed at 20 °C. Creep and recovery tests were performed at different shear stresses during the creep period. Five values have been selected: 4, 6, 8, 10 and 12 Pa. The duration of the creep and the recovery parts was kept constant at 100 s and 200 s, respectively. An example for a job (procedure) setup for a creep and recovery test with the Thermo Scientific™ HAAKE™ RheoWin™ Job Manager is shown in Figure 4.

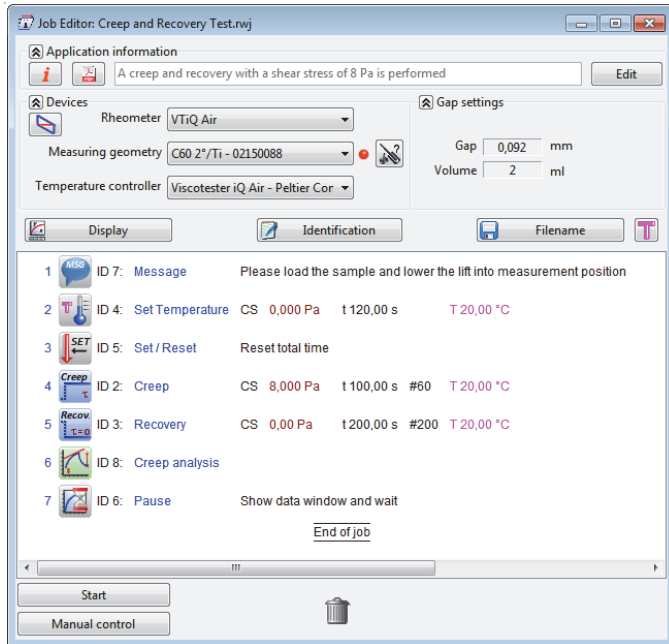


Fig. 4: Thermo Scientific HAAKE RheoWin routine for a creep and recovery test including data evaluation.

Results and discussions

The results of creep and recovery tests with the cosmetic emulsion performed with different stresses are shown in Figure 5. It can be seen, that the sample behaves like a viscoelastic material with an instantaneous deformation (elastic response) once the stress is applied followed by a delayed viscoelastic deformation. When the stress is removed the sample generates a back deformation due to its elasticity and the energy stored during the creep period. It can be seen that the percentage of recoverable deformation is decreasing with increasing shear stress. Table 1 reports the numerical values of percentage of recoverable deformation as directly calculated by the RheoWin creep and recovery evaluation routine.

Table 1: Percentage of recoverable deformation for different stresses during the creep phase.

Shear stress during creep phase (Pa)	Percentage recoverable deformation (%)
12	23.78
10	53.13
8	70.77
6	79.80
4	76.67

For a better comparability of the different runs and to identify major changes in the deformation behavior it is helpful to plot the compliance instead of deformation as a function of time. The compliance is defined as the ratio of the deformation, γ and the applied stress, τ :

$$J = \gamma / \tau \quad [2]$$

Such a plot is shown in Figure 6.

It can be seen that the results of the experiments with a shear stress of 4 and 6 Pa overlay in the compliance versus time plot. This behavior is indicating that the applied stresses in the creep phase are still below the yield stress τ_0 of the tested material. The yield stress is considered the minimum shear stress required to overcome elastic deformation of a material and to generate flow. Above the shear stress of 6 Pa the curves are differing and at 12 Pa a clear linear increase of compliance over time occurs. This is indicating that the yield stress of the sample is exceeded and flow is induced.

The equilibrium compliances values as directly calculated by the RheoWin software are shown in Table 2.

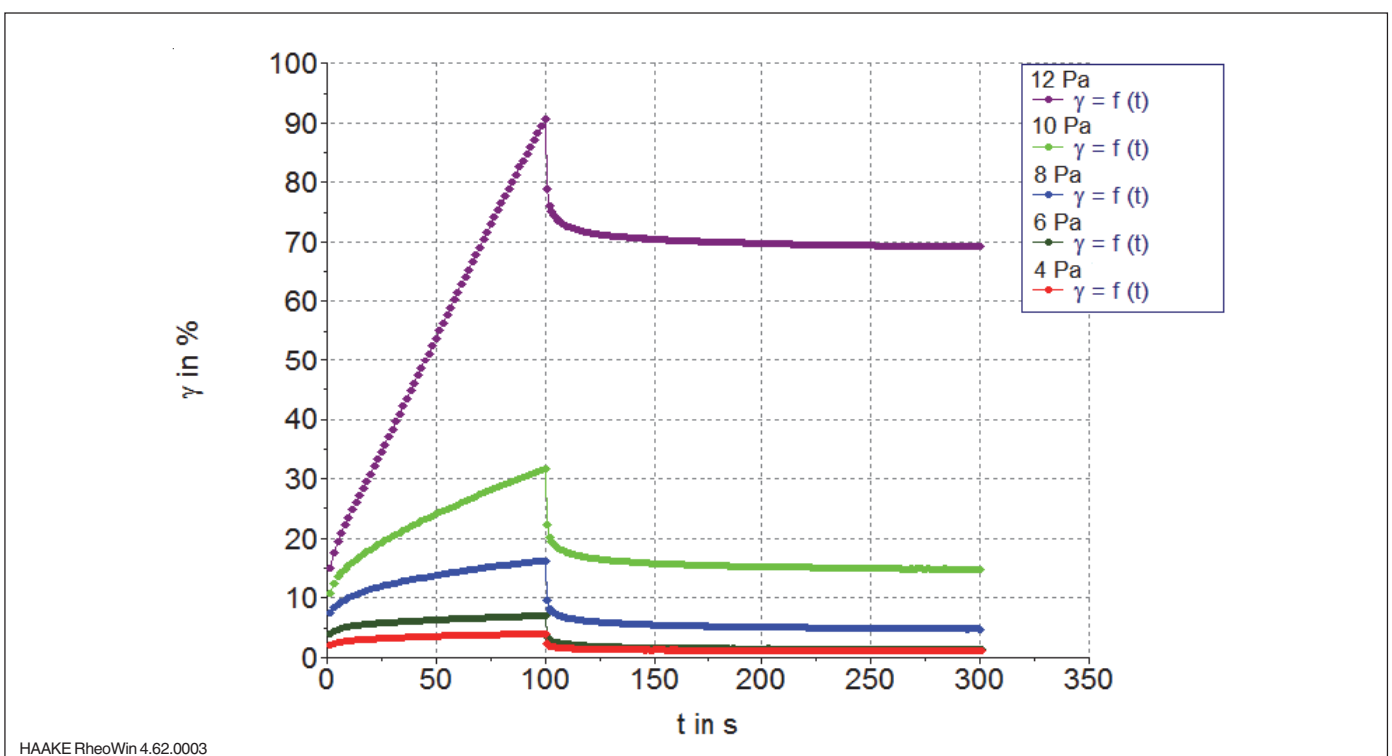


Fig. 5: Creep and recovery test with cosmetic emulsion at different shear stress.

Table 2: Equilibrium compliance for different stresses during the creep phase.

Shear stress during creep phase (Pa)	Equilibrium compliance (1/Pa)
12	0.01683
10	0.01702
8	0.01628
6	0.01156
4	0.01109

At shear stresses of 6 and 8 Pa the values of the equilibrium compliance are smaller than at higher stresses. This is probably due to the fact that at the low shear

stresses the duration of the creep phase was not long enough to reach the steady state and the elastic components of the sample were not fully stretched yet. On the opposite, at the higher stresses the duration of the creep phase was long enough to reach steady state flow and the calculated values of the equilibrium compliance are, within a certain tolerance, independent of the applied stress.

A standard determination method of the yield stress consists in performing a stress ramp experiment. In this test a linearly increasing shear stress is applied and the deformation of the sample is monitored over time. The result of the stress ramp experiment with the same cosmetic emulsion used for the creep and recovery tests is shown in Figure 7.

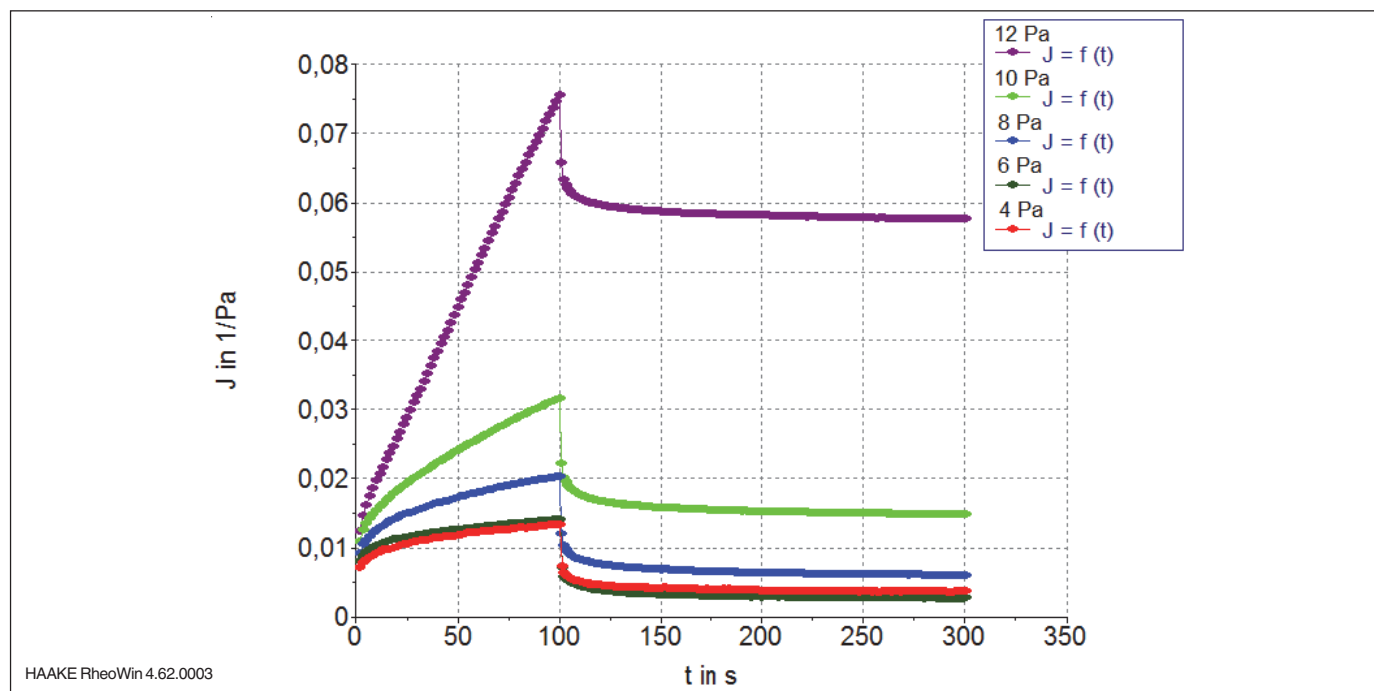


Fig. 6: Creep and recovery test with cosmetic emulsion with different shear stress values during the creep phase.

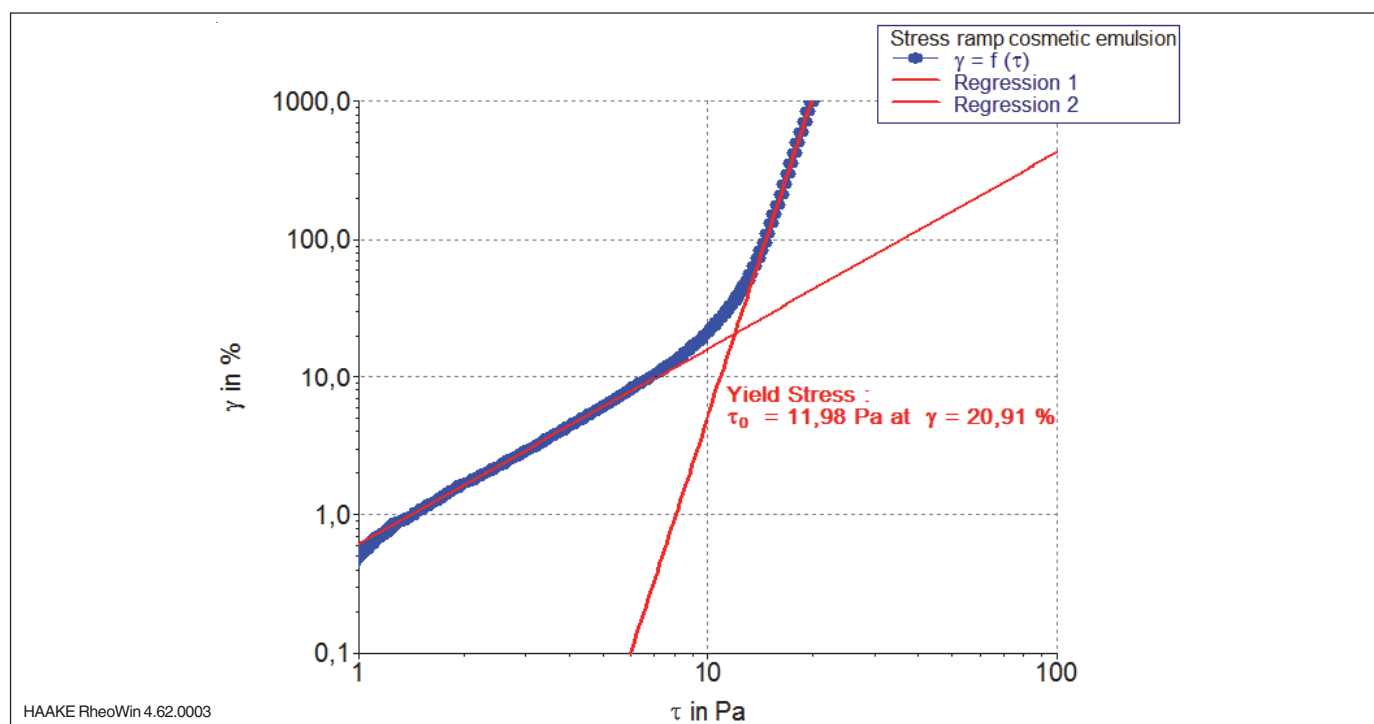


Fig. 7: Stress ramp test with yield stress determination according to tangent method for cosmetic emulsion.

The deformation stress curve shows 3 distinct regions. In the first region (i.e. below the yield stress) the sample is deformed elastically by the applied stress. Here the slope of the deformation stress curve is not much larger than 1 in the double logarithmic plot. As the stress increases and approaches the yield stress of the sample, the deformation starts to change more rapidly and the slope increases. At higher shear stresses a second linear region with a higher slope is observed. Here the sample is flowing. A common way to calculate the yield stress using the data collected during a shear stress experiment is the tangent method. The yield stress corresponds to the stress value at the intersection of the tangents to the two linear regions. The yield stress

of the cosmetic emulsion according to this method is around 12 Pa. This value is higher than the yield stress estimated from the creep and recovery tests. This difference can be explained by the fact that the intersection of the tangents generates a value which falls into the transition region where the materials behavior is not entirely elastic anymore. The true onset of flow can be obtained when plotting viscosity versus shear stress as shown in Figure 8.

The viscosity curve shows a maximum at 5.5 Pa. In Figure 9 the viscosity data were plotted together with the deformation data on the same graph.

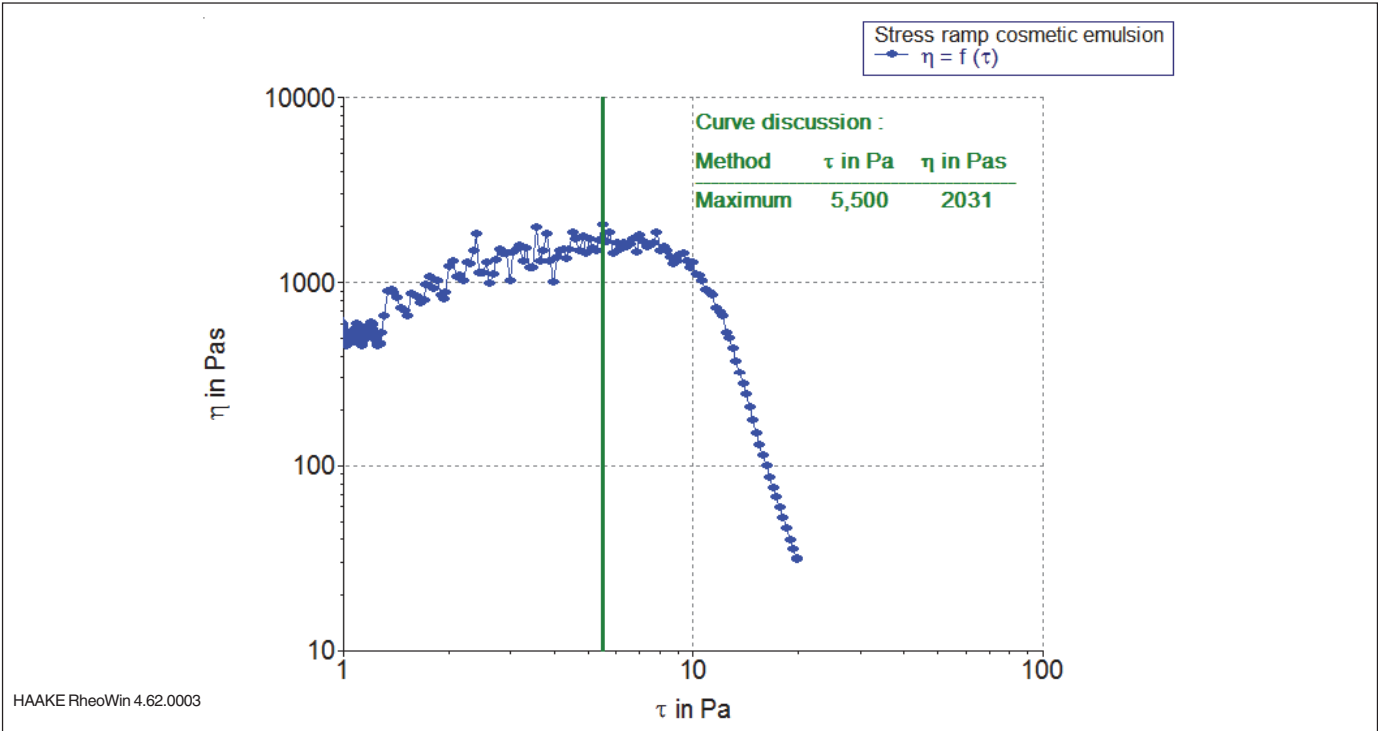


Fig. 8: Viscosity as a function of shear stress for cosmetic emulsion with determination of maximum viscosity.

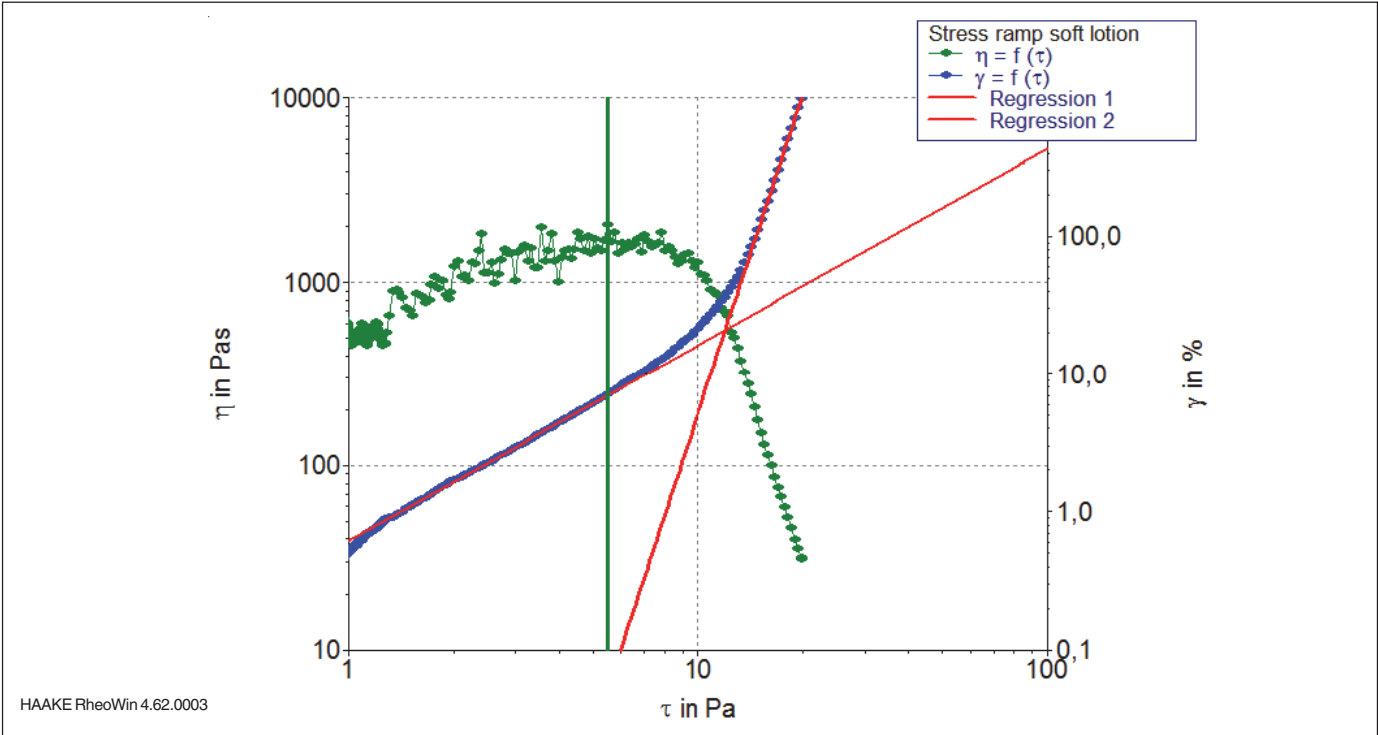


Fig. 9: Viscosity as a function of shear stress for cosmetic emulsion with determination of maximum viscosity.

It can be observed that the maximum in viscosity occurs when the deformation enters the transition range. This stress value is in good agreement with a yield stress of 6 Pa derived from the creep and recovery tests.

Conclusions

It was demonstrated that the HAAKE Viscotester iQ Air can be used to perform creep and recovery tests even on weakly structured viscoelastic samples. Creep and recovery tests are not only a useful rheological method to differentiate and quantify the viscous and elastic properties of a material but can also be used to measure yield stresses very accurately.

Find out more at thermofisher.com/rheometers

The logo for ThermoFisher Scientific, with "ThermoFisher" in red and "SCIENTIFIC" in black.

APPLICATION NOTE

Performing quality control (QC) tests on cosmetic emulsions with the HAAKE Viscotester iQ rheometer

Authors

Klaus Oldörp

Thermo Fisher Scientific, Karlsruhe, Germany

Introduction

The formulation of a cosmetic product can be quite complex and will vary depending on the active ingredients. Still, the customer expects a cream from a certain product range always to have the same texture, no matter the particular ingredients like for example aloe vera, lemon grass or milk and honey. Subsequently, one of the challenges when formulating a cosmetic product is to achieve the texture the customer expects or desires. Testing the rheological properties of a cosmetic emulsion therefore is an essential part of such a product's quality control (QC).

Typical rheological parameters tested for cosmetic emulsion are the shear viscosity η , the thixotropic behaviour and the yield stress τ_0 . The viscosity is related to various product properties depending on the shear rate range in question. For example, the feel of a cream when rubbing it into the skin is linked to the viscosity at higher shear rates, while the storage stability is related to its viscosity at low shear rates.

The yield stress of an emulsion is important for the storage stability and the look and feel of the product. A cream sold in a pot will have higher yield stress because the customer expects to be able to take a bit of cream out of the pot with his finger. A body lotion is filled in bottles and the customer expects a liquid-like behaviour. Thus this products needs to have a relatively low yield stress.

To be able to test these different rheological parameters, a QC viscometer needs to offer a variety of test methods and a broad measuring range. To make rheological tests in QC easier and more reliable, the Thermo Scientific™ HAAKE™ Viscotester™ iQ rheometer has been developed. This unique viscometer has some features especially designed for QC applications. For example, due to its improved sensitivity it is possible to use smaller cylindrical measuring geometries and even parallel plate geometries, thus reducing sample volume, time required for temperature equilibration and cleaning effort.

**Methods and materials**

A soft cream and a body lotion have been selected for the test described in this report. To reduce the damage to the emulsion's structure during sample loading, the tests were carried out using a 35 mm parallel plate geometry with a 1 mm gap. Compared to a cylindrical measuring geometry this reduces the sample volume to about 1 ml and helps saving time by allowing much easier cleaning of the geometry after each test.

Before the tests a small amount of sample was placed onto the lower exchangeable plate sitting on the Peltier temperature control unit of the HAAKE Viscotester iQ. The upper plate was lowered carefully by hand down to the measuring gap in order to minimize the preshearing of the samples. Finally a sample cover was put over the closed measuring geometry to improve temperature control and to minimize evaporation.

The HAAKE RheoWin Job

After lowering the upper plate, the HAAKE Viscotester iQ rheometer was operated using the Thermo Scientific™ HAAKE™ RheoWin™ software.

The first part of the HAAKE RheoWin job is the sample conditioning. For the emulsions tested here it simply consists of a waiting period to give the samples enough time to relax the mechanical stress from sample loading and to bring it to the test temperature. Even though it is “just” a waiting period, the sample conditioning should always be part of the test method itself to ensure that it is not forgotten and always performed in the same way, which improves the reproducibility of the results.

The next part of the HAAKE RheoWin job is the rheological test itself. The last part usually consists of the data evaluation, the generation of a report and its printout or export if required.

Results and discussion

The viscosity is best tested by recording the steady-state viscosity curve i.e. the steady-state viscosity as a function

of shear rate. Compared to transient viscosity data from shear rate ramps, the steady-state viscosity is independent from time-dependent effect and the slope of the shear rate ramp. For comparison of viscosity data the steady-state viscosity is the best choice, because it is independent of the instrument used and can be correlated with the shear rate applied.

Within the almost four orders of magnitude in shear rate covered during the test, both viscosity curves displayed in Figure 2 show a pronounced shear thinning behaviour. As expected, the soft cream has the higher viscosity at low shear rates but it also shows the stronger shear thinning. Within the range of these measurements, the viscosity of the soft cream drops by a factor of almost 500, while the viscosity of the body lotion only drops by a factor of 120.

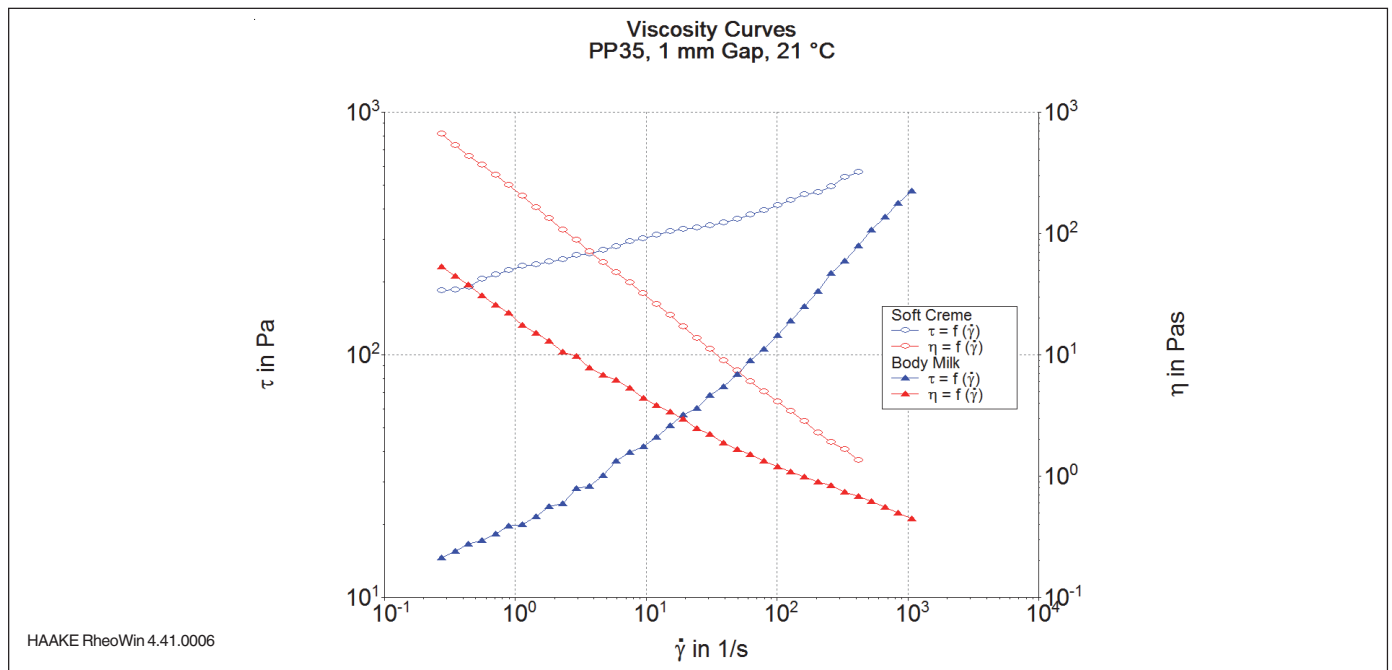


Fig. 2: Viscosity curves (red) and flow curves (blue) of a soft cream (open symbols) and a body lotion (filled symbols). The soft cream shows the higher viscosities and the stronger shear thinning.

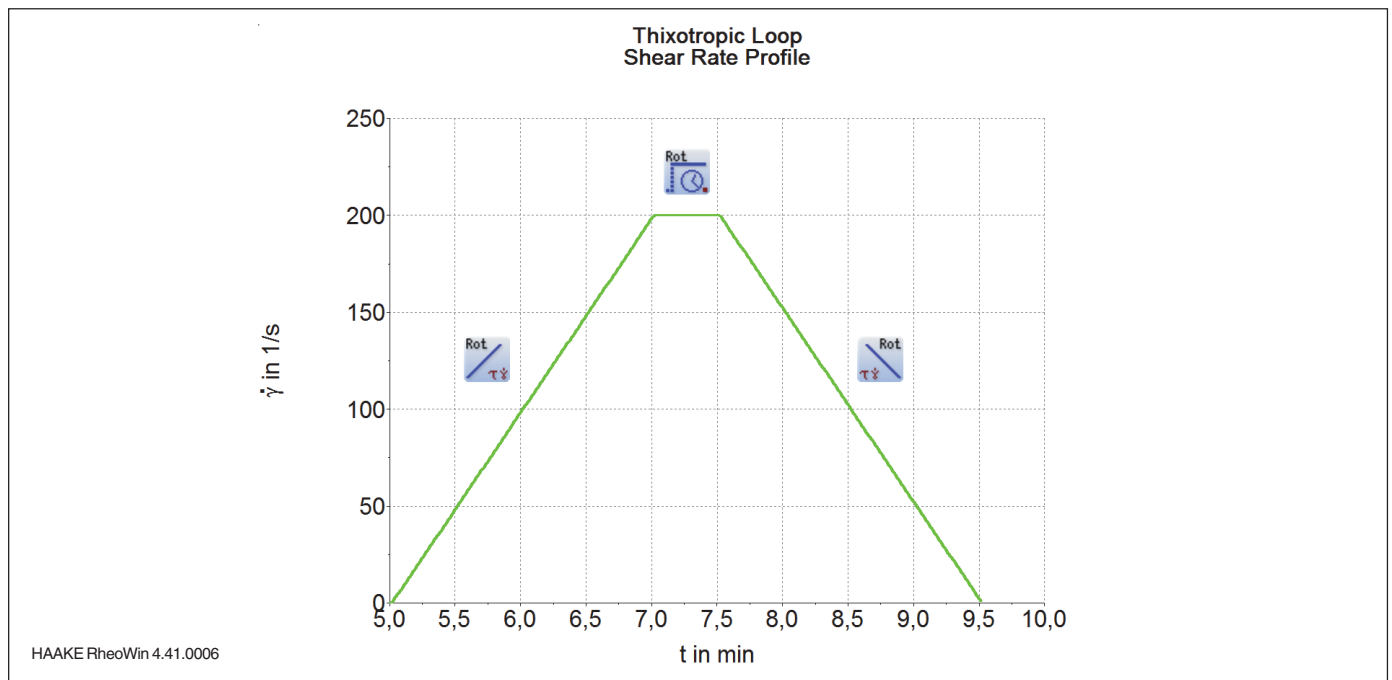


Fig. 3: Shear rate profile for the so-called “thixotropy loop” consisting of an up ramp, a peak hold time at the maximum shear rate and a down ramp.

Extrapolating both viscosity curves to higher shear rates predicts that the viscosity of both products will be identical at approximately 2000 s^{-1} . This similarity is not accidental because rubbing a cream or lotion into the skin happens in that range of shear rate and the viscosity, which is felt as being pleasant on the skin, is of course the same for both products.

Thixotropy

In QC, the thixotropic behaviour is usually tested with the so-called “thixotropy loop“. The advantage of this test method is the short time the test takes compared to other commonly used methods.

The test consists of 3 elements: A shear rate ramp from 0 s^{-1} up to the maximum shear rate (in this case 200 s^{-1}), an element keeping the maximum shear rate constant over some time and a second shear rate ramp going back to 0 s^{-1} (Figure 3). Usually the durations of the up ramp and down ramp are identical. The time for the constant shear element should be long enough for the sample to reach a constant viscosity before starting the down ramp.

The results of these tests are evaluated by calculating the area between the flow curves from the up ramp and the down ramp. The bigger the area, the stronger the thixotropy of the sample.

One important fact to keep in mind: the result of this test depends on the test parameters, i.e. the maximum shear rate and the slope of the ramps. Only if the shear rate profile (like e.g. shown in Figure 3) is kept the same, results from different tests can be compared.

Running this test on both samples gave a significant difference in the results. While the soft cream clearly showed a thixotropic behaviour (Figure 4, open symbols), the body lotion showed no thixotropy at all.

Yield stress

If a material has a yield stress, it behaves like an elastic solid when exposed to a shear stress below the yield stress and like a viscous liquid when the stress applied is higher than the yield stress. Therefore, the recommended method to test, whether a sample has a yield stress and at which stress value it appears, is a linear continuous increase of the applied stress [1].

For the evaluation of the test results, the deformation of the sample is plotted as a function of the stress applied. For the determination of the yield stress, only the first discontinuity in the deformation curve can be used. Similar points at higher stresses are related to other changes of structure in the sample. Straight lines are fitted to the linear parts (in the double logarithmic plot) of the deformation curve below and above the first discontinuity. The yield stress is calculated from the point of intersection of these two straight lines (Figure 5).

With this method, data below as well as above the yield stress is recorded. Thus, no extrapolation is needed, which increases the reproducibility and reliability of calculated value for the yield stress considerably.

While the body lotion showed no yield stress within the range of measurement, the soft cream showed a distinct yield stress of 110 Pa (Figure 5).

Conclusion

The HAAKE Viscotester iQ rheometer is a compact instrument with the right combination of sensitivity and strength to successfully test a wide range of samples with different QC methods in controlled rate (CR) or controlled stress (CS) mode. The sensitivity of the instrument allows covering a wide range of shear rates with only one measuring geometry. For cosmetic emulsions, the parallel plate geometry proved

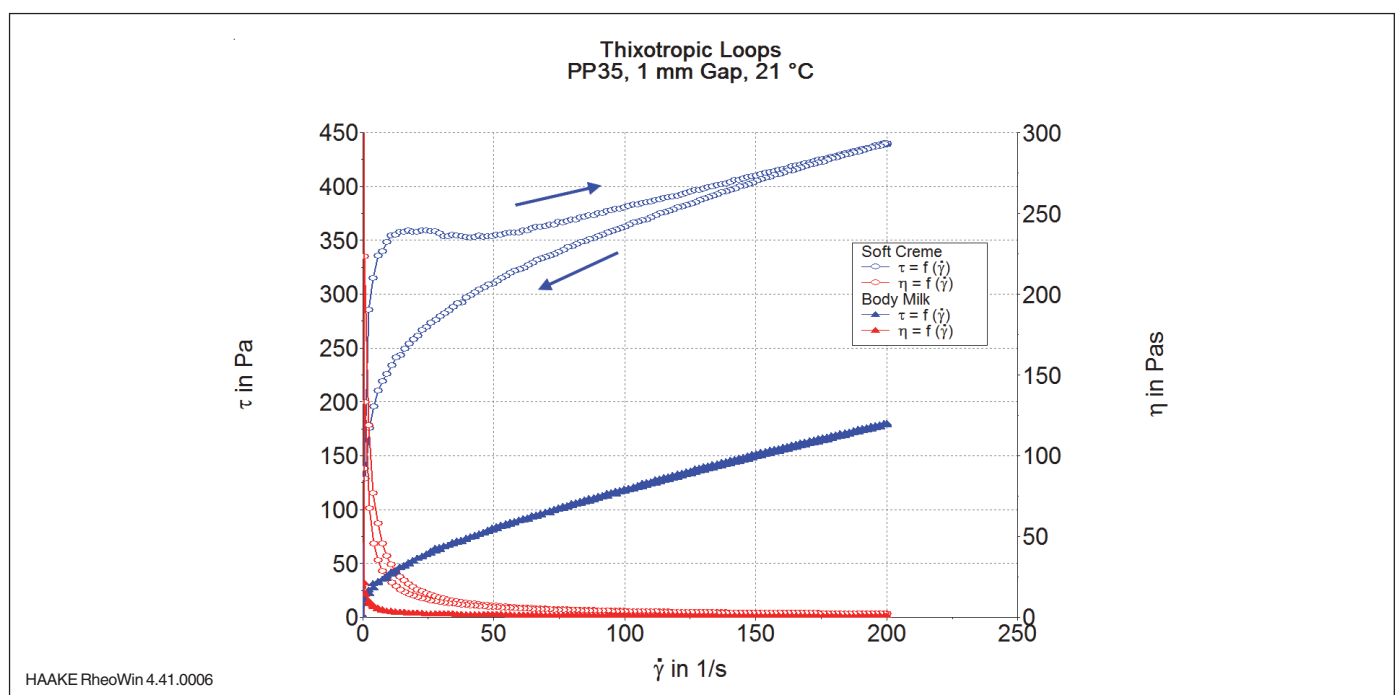


Fig. 4: Results of the thixotropy test for soft cream (open symbols) and body lotion (filled symbols). The soft cream shows a thixotropic behaviour, indicated by the clear difference between the up and down part of the flow curve. The up and down curve for the body lotion are identical, thus the sample is not thixotropic.

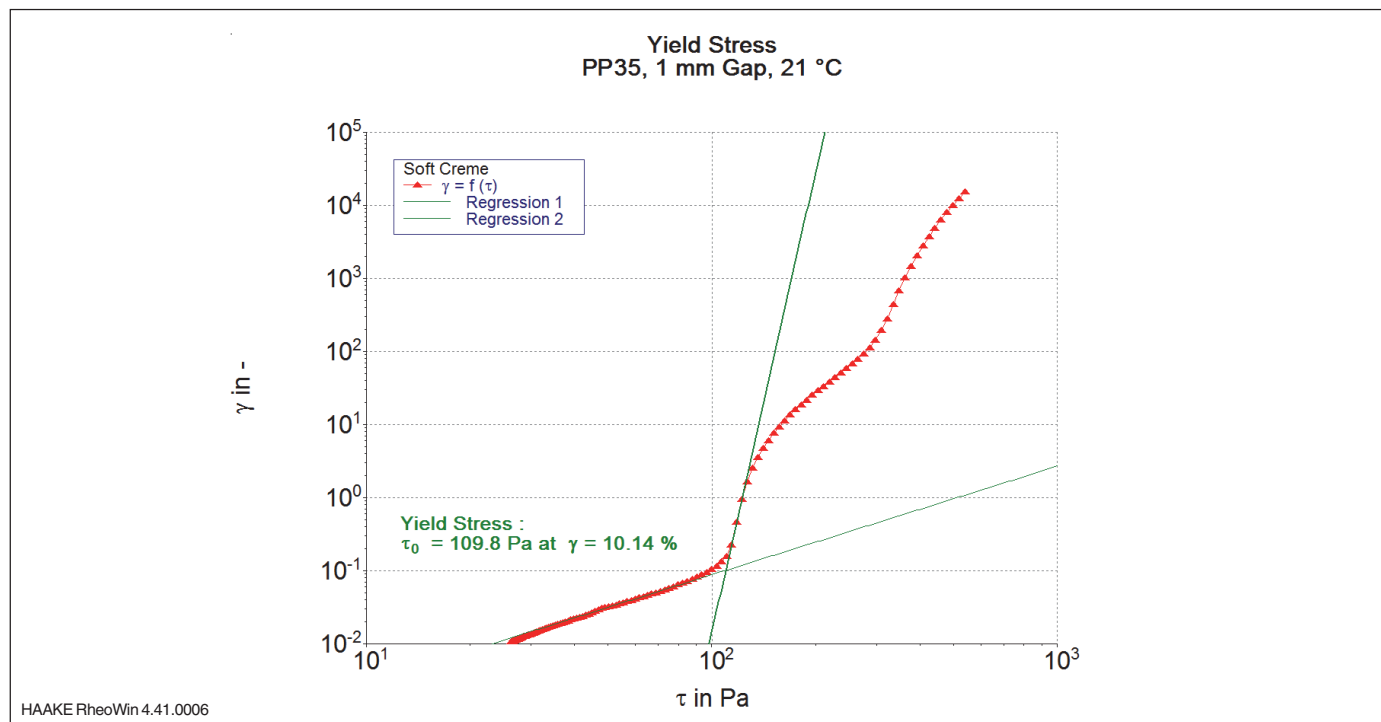


Fig. 5: Deformation as a function of stress for the soft cream sample. The yield stress is calculated as the point of interception of the two green tangents, marking the transition from elastic deformation to viscous flow.

to be particularly useful since its use reduces the stress on the sample during sample loading. In addition, it significantly reduces the time between tests due to a much simpler and therefore faster cleaning procedure.

The very good quality of the results shown in this report is an excellent base for a reliable data analysis with a variety of available methods and models.

Reference

- [1] DIN Technical Report No. 143 of the NPF/NAB-AK 21.1
"Rheology" (Pigments and extenders)

Find out more at thermofisher.com/rheometers

ThermoFisher
SCIENTIFIC

Quality control of industrial dye products using absorbance spectroscopy

Key Words

NanoDrop spectrophotometer, absorbance, industrial dyes, quality control (QC), uranine

Introduction

Quality control of industrial dye additives is imperative to ensure the reproducibility of dye color and appearance in the colorant's final application. The Thermo Scientific™ NanoDrop™ 2000 UV-Vis spectrophotometer offers a rapid, fully customizable method for checking batch quality for proper pigment concentration prior to distribution to the product's end user. The concentrations of most aqueous dyes and pigments can be assessed using the full ultraviolet and visible spectrum capabilities of the NanoDrop 2000 spectrophotometer.

The NanoDrop 2000 spectrophotometer utilizes autoranging pathlengths to quantify dye samples across a much broader concentration range than is possible using a conventional cuvette-based spectrophotometer. By optimizing the pathlength based on dye absorbance (ranging from 1.0 mm to 0.05 mm) the NanoDrop 2000 spectrophotometer can accurately measure the absorbance of a sample across a concentration range nearly 200 fold greater than that of a cuvette-based system.

In this study, the visible absorbance spectrum of uranine, the disodium salt of fluorescein, was assessed using a NanoDrop 2000 spectrophotometer across a broad concentration range. Uranine is commonly used in oil and gas industries to detect leaks in containment vessels and pipelines. It is also used as a colorant in military, medical, and cosmetic applications. Both linear dynamic range and precision (reproducibility) were assessed.

Experimental Procedures

The absorbance of uranine test samples was measured at 490 nm. A custom method was developed in the NanoDrop 2000 software that allowed for ideal lamp integration times for analysis of the peak of interest (Figure 1), while avoiding additional peaks in the UV region of the spectrum.

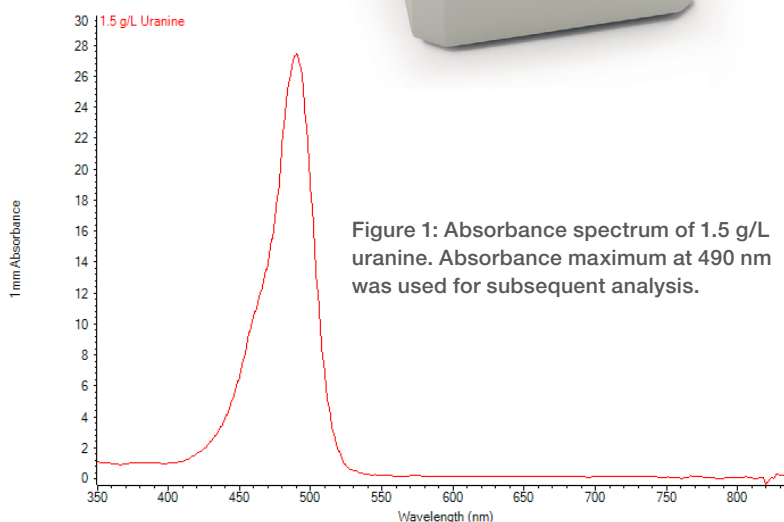


Figure 1: Absorbance spectrum of 1.5 g/L uranine. Absorbance maximum at 490 nm was used for subsequent analysis.

A 1.5 g/L stock solution was prepared by dissolving 1.5 g uranine powder in 20 mL of 1 N sodium hydroxide. Volume was adjusted to 1 L in a volumetric flask using deionized water. Linear dynamic range was tested by measuring a serial dilution of this stock solution. Absorbance of five, 2.0 μ L aliquots of each dilution were measured at 490 nm using a custom method developed using the Method Editor in the NanoDrop 2000 software.

Results

A linear relationship between absorbance and dye concentration was observed throughout the concentration range measured (Figure 2).

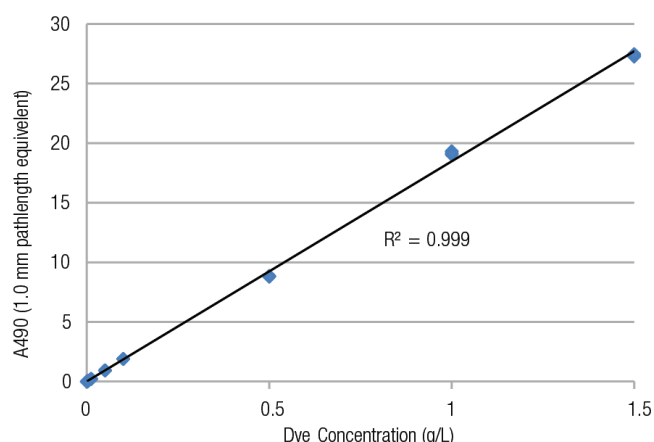


Figure 2: Uranine absorbance vs. concentration at 490 nm. Strong linear response observed through the entire dilution range.

Reported absorbances at 490 nm ranged from 0.02 A at the lowest concentration (0.0015 g/L) to over 27 A for the highest (1.5 g/L) concentration solution at a 1.0 mm pathlength equivalent.

Reproducibility across replicate aliquots was very good; CV values of 1% or less were observed in samples above 0.003 g/L, with excellent standard deviations in all cases (Table 1). This data indicates a linear, reproducible measurement range nearly 200 times broader than a traditional spectrophotometer utilizing a 1 cm cuvette.

Concentration (g/L)	Average A490	SD	% CV
0	0.000	0.001	
0.0015	0.021	0.001	
0.003	0.046	0.002	
0.012	0.220	0.002	1.045
0.050	0.936	0.005	0.507
0.100	1.895	0.007	0.389
0.500	8.832	0.033	0.370
1.000	19.185	0.124	0.648
1.500	27.367	0.091	0.333

Table 1: Average, standard deviation, and % CV of replicate aliquots (n = 5) of a serial dilution of uranine dye.

Conclusion

The use of UV-Visible spectrophotometers for the quality control of dyes and pigments has been a standard practice for decades. However, the detection limitations of a fixed-pathlength, cuvette-based spectrophotometer require that a pigment sample be heavily diluted prior to measurement. These dilutions introduce a potential source of error in the quality control process. The NanoDrop 2000 UV-Vis spectrophotometer can be employed to provide a rapid and accurate verification of dye concentration without the need for significant dilutions. The custom method capabilities of the NanoDrop 2000 software can be used to develop specific applications for various dyes and pigment quality processes, allowing data capture and analysis to be performed automatically. The polished stainless steel and quartz construction of the measurement pedestal is highly resistant to sample carryover or staining, even when exposed to extremely concentrated dyes. In addition, the instrument's short measurement cycle, lack of a warm-up period, and general ease of use greatly increases the rate at which samples can be processed.

Find out more at www.thermofisher.com

ThermoFisher
SCIENTIFIC

Customer Service

We are committed to delivering top-notch customer support, including tailored service products and fast response times. We offer a comprehensive range of services that can quickly and flexibly respond to various service needs and requests.

Application Laboratories and Support

Our fully equipped application laboratories are in constant demand for testing customer samples, and developing and optimizing pioneering applications. We also provide a broad range of product and application solutions, and our team of application specialists is on hand to answer your questions.

Seminars, Training Courses and Webinars

You will find comprehensive training programs, in-house seminars, and practical courses for extrusion, spectroscopy and rheology in various locations around the world.

Find out more at

www.thermofisher.com/cosmetics

www.thermofisher.com/extrusion

www.thermofisher.com/spectroscopy

www.thermofisher.com/rheology